Dear Author,

Please, note that changes made to the HTML content will be added to the article before publication, but are not reflected in this PDF.

Note also that this file should not be used for submitting corrections.

AUTHOR QUERY FORM

ELSEVIER	**Journal: OREGEO** **Article Number: 1362**	**Please e-mail or fax your responses and any corrections to:** **Moorthy, Hemalatha** **E-mail: Corrections.ESCH@elsevier.spitech.com** **Fax: +1 619 699 6721**

Dear Author,

Please check your proof carefully and mark all corrections at the appropriate place in the proof (e.g., by using on-screen annotation in the PDF file) or compile them in a separate list. Note: if you opt to annotate the file with software other than Adobe Reader then please also highlight the appropriate place in the PDF file. To ensure fast publication of your paper please return your corrections within 48 hours.

For correction or revision of any artwork, please consult http://www.elsevier.com/artworkinstructions.

We were unable to process your file(s) fully electronically and have proceeded by

☐ Scanning (parts of) your article ☐ Rekeying (parts of) your article ☐ Scanning the artwork

Any queries or remarks that have arisen during the processing of your manuscript are listed below and highlighted by flags in the proof. Click on the 'Q' link to go to the location in the proof.

Location in article	Query / Remark: click on the Q link to go Please insert your reply or correction at the corresponding line in the proof
Q1	Citation "Carvalho, 1976" has not been found in the reference list. Please supply full details for this reference.
Q2	Please confirm that given names and surnames have been identified correctly.
Q3	Highlights should consist of only 125 characters per bullet point, including spaces. However, the Highlights provided for this item exceed the maximum requirement. Kindly provide replacement Highlights that conform to the requirement for us to proceed. For more information, please see the Guide for Authors.
Q4	One parenthesis has been deleted to balance the delimiters. Please check that this was done correctly, and amend if necessary.
Q5	Citation "Leblanc et al., 2000" has not been found in the reference list. Please supply full details for this reference.
Q6	The citation "Routhier et al. (1980)" has been changed to match the author name/date in the reference list. Please check here and in subsequent occurrences, and correct if necessary.
Q7	The citation "Sáez et al. (1996, 1999)" has been changed to match the author name/date in the reference list. Please check here and in subsequent occurrences, and correct if necessary.
Q8	Citation "Sánchez et al., 1996" has not been found in the reference list. Please supply full details for this reference.
Q9	The citation "Álvaro et al., 2002" has been changed to match the author name/date in the reference list. Please check here and in subsequent occurrences, and correct if necessary.

Q10	One parenthesis has been added to balance the delimiters. Please check that this was done correctly, and amend if necessary.
Q11	Citation "Quesada, 1991" has not been found in the reference list. Please supply full details for this reference.
Q12	Citation "Van den Boogaard and Schermerhörn, 1975" has not been found in the reference list. Please supply full details for this reference.
Q13	The citation "Sáez et al., 1996" has been changed to match the author name/date in the reference list. Please check here and in subsequent occurrences, and correct if necessary.
Q14	Citation "Tornos and Heinrich, 2008" has not been found in the reference list. Please supply full details for this reference.
Q15, Q27	Citation "González et al., 2000" has not been found in the reference list. Please supply full details for this reference.
Q16, Q28	The citation "Nieto et al., 2002" has been changed to match the author name/date in the reference list. Please check here and in subsequent occurrences, and correct if necessary.
Q17	Citation "Sáez et al., 1996" has not been found in the reference list. Please supply full details for this reference.
Q18	The citation "Sierro, 1990" has been changed to match the author name/date in the reference list. Please check here and in subsequent occurrences, and correct if necessary.
Q19	Citation "Sala, 1984" has not been found in the reference list. Please supply full details for this reference.
Q20, Q31	The citation "Moreno et al., 2003" has been changed to match the author name/date in the reference list. Please check here and in subsequent occurrences, and correct if necessary.
Q21, Q23	The citation "Tornos et al., 2006" has been changed to match the author name/date in the reference list. Please check here and in subsequent occurrences, and correct if necessary.
Q22	The citation "Lagoa Salgada, Oliveira et al., 2011" has been changed to match the author name/date in the reference list. Please check here and in subsequent occurrences, and correct if necessary.
Q24	Citation "Tornos et al., 2008" has not been found in the reference list. Please supply full details for this reference.
Q25	Citation "García Palomero (1992)" has not been found in the reference list. Please supply full details for this reference.
Q26	Citation "García Palomero, 1992" has not been found in the reference list. Please supply full details for this reference.
Q29	Citation "Sáez et al., 2011" has not been found in the reference list. Please supply full details for this reference.
Q30	The citation "Simancas et al., 2003" has been changed to match the author name/date in the reference list. Please check here and in subsequent occurrences, and correct if necessary.
Q32	The citation "Abad et al., 2007" has been changed to match the author name/date in the reference list. Please check here and in subsequent occurrences, and correct if necessary.
Q33	The citation "Meléndez-Hevia et al., 1996" has been changed to match the author name/date in the reference list. Please check here and in subsequent occurrences, and correct if necessary.
Q34, Q36	The citation "Hoefs, 1996" has been changed to match the author name/date in the reference list. Please check here and in subsequent occurrences, and correct if necessary.

Q35	Citation "Nuzzo et al. (2009)" has not been found in the reference list. Please supply full details for this reference.
Q37	Uncited references: This section comprises references that occur in the reference list but not in the body of the text. Please position each reference in the text or, alternatively, delete it. Thank you.
Q38	Please provide the corresponding grant number for the grant sponsor "Spanish Government (MINECO)". Please check this box if you have no corrections to make to the PDF file. ☐

Thank you for your assistance.

Ore Geology Reviews xxx (2014) xxx

Contents lists available at ScienceDirect

Ore Geology Reviews

journal homepage: www.elsevier.com/locate/oregeorev

Highlights

Ore Geology Reviews xxx (2014) xxx–xxx

The Las Cruces deposit, Iberian Pyrite Belt, Spain

Lola Yesares [a,*], Reinaldo Sáez [a], José Miguel Nieto [a], Gabriel Ruiz De Almodóvar [a], Carmelo Gómez [b], Juan Manuel Escobar [b]

[a] Department of Geology, University of Huelva, Avenida de las Fuerzas Armadas, S/N, 21071 Huelva, Spain
[b] Geological Area, Mining Department of Cobre Las Cruces S.A., Ctra. SE-3410, Km 41, 100, 41860 Gerena, Seville, Spain

- First report of geology, structure, geochemistry and mineralogy of the Las Cruces different deposit sectors.
- Genetic model that explains the origin of the Las Cruces primary sulfides and the evolution of the supergene profile is proposed.
- Comparison with other VMS deposits and their supergene profiles.
- The role of carbonated sedimentary cover and the water–rock interaction processes.

Q3

http://dx.doi.org/10.1016/j.oregeorev.2014.10.019
0169-1368/

Please cite this article as: Yesares, L., et al., The Las Cruces deposit, Iberian Pyrite Belt, Spain, Ore Geol. Rev. (2014), http://dx.doi.org/10.1016/j.oregeorev.2014.10.019

Ore Geology Reviews xxx (2014) xxx–xxx

Contents lists available at ScienceDirect

Ore Geology Reviews

journal homepage: www.elsevier.com/locate/oregeorev

The Las Cruces deposit, Iberian Pyrite Belt, Spain

Lola Yesares [a,*], Reinaldo Sáez [a], José Miguel Nieto [a], Gabriel Ruiz De Almodóvar [a], Carmelo Gómez [b], Juan Manuel Escobar [b]

[a] Department of Geology, University of Huelva, Avenida de las Fuerzas Armadas, S/N, 21071 Huelva, Spain
[b] Geological Area, Mining Department of Cobre Las Cruces S.A., Ctra. SE-3410, Km 41, 100, 41860 Gerena, Seville, Spain

ARTICLE INFO

Article history:
Received 21 January 2014
Received in revised form 20 October 2014
Accepted 21 October 2014
Available online xxxx

Keywords:
Las Cruces deposit
Iberian Pyrite Belt
Supergene enrichment
Gossan

ABSTRACT

The Las Cruces deposit is located at the eastern margin of the Iberian Pyrite Belt (IPB), beneath the Neogene-Quaternary deposits of the Guadalquivir Basin. These sediments covered and preserved the supergene profile somewhat after its generation until its recent discovering. For this reason, the Las Cruces ore deposits, together with Lagoa Salgada in Portugal, are the only known deposits in the IPB that preserve the entire weathering profile, including both the gossan and the enrichment zone. In that sense, the present study provides new data on the IPB ore deposits and their post-Palaeozoic evolution.

The primary mineralization consists of massive and semi-massive polymetallic sulfides overlaying a cupriferous and pyritic stockwork. The supergene enrichment extends from the primary zone to gossan and consists of a thick cementation zone characterized by intense replacement of part of the primary sulfides by Cu-rich supergene sulfides.

At present, the only economic resource of Las Cruces is the cementation zone, with initial reserves of 17.6 Mt @ 6.2% Cu, but the orebody also includes significant contents of Cu and Zn within the primary mineralization, and Au, Ag, and Pb in the gossan.

Mineralogical and geochemical data confirm that the primary mineralization at Las Cruces resembles other IPB deposits in terms of distribution and evolution, however the gossan and cementation zone show an uncommon evolution for this kind of supergene profile. The major singularity that makes the Las Cruces supergene mineralisation noticeably different from others in the IPB or elsewhere resides in its unusual mineralogical composition, mostly comprised of newly-formed siderite, calcite, Fe-sulfides and galena.

The genetic model proposed for the Las Cruces deposit includes three main stages: (1) ore genesis and evolution of primary mineralization, which seems to be comparable to other IPB deposits; (2) genesis of Cu-rich secondary mineralization and gossan by weathering, after Miocene exhumation, of the upper part of the massive sulfide deposit, under oxidizing and acidic conditions; and (3) late evolution of supergene profile below the carbonated-rich sediments of the Guadalquivir Basin, with the subsequent change in the redox conditions due to water–rock interaction between the supergene profile and basinal fluids.

1. Introduction

The Las Cruces orebody is located at the eastern corner of the Iberian Pyrite Belt (IPB), 25 km northwest of Seville (Spain), and it is covered by a detrital and carbonate sequence, 150-m-thick, of the Guadalquivir foreland Basin.

The Las Cruces deposit included a polymetallic massive sulfide orebody and a Cu-rich stockwork. In the upper sector it includes a supergene profile containing a gossan above a cementation zone, which represents the current economic resource.

The Las Cruces deposit, discovered in 1992 by Riomin Exploraciones S.A., is currently mined by open pit by Cobre Las Cruces S.A., a local subsidiary of First Quantun Minerals. Current mining operation only includes the cementation zone, with initial reserves of 17.6 Mt @ 6.2% Cu. The remaining reserves at 31st December 2012 are 14.1 Mt @ 5.4% Cu. In addition, the deposit also includes important resources in the supergene profile (2 Mt of gossan ore @ 4.5% Pb, 5.1 g/t Au and 115 g/t Ag) and base metals in the massive sulfide orebody (4.5 Mt of Cu-rich ore @ 3.3% Cu and 20.7 Mt of polymetallic-rich ore @ 4.2% Zn and 2% Pb) (Doyle et al., 2003).

The IPB is one of the most prolific massive sulfide provinces on Earth (Sáez et al., 1999). It hosts more than 100 inactive or working mines, and includes 22% (14) of the world class VMS deposits (Tornos, 2006). Of these, eight deposits (Riotinto, Tharsis, La Zarza, Sotiel, Masa Valverde and Aznalcollar in Spain, and Neves Corvo and Aljustrel in Portugal) have been classified as giants (>100 Mt). The IPB contains original reserves above 1700 Mt (Carvalho et al., 1999; Leistel et al., 1998), and even after 4.5 ka of continuous metal extraction (Leblanc et al., 2000; Sáez et al., 2003; Nocete et al., 2005), it still hosts

* Corresponding author.
E-mail address: lola.yesares@dgeo.uhu.es (L. Yesares).

http://dx.doi.org/10.1016/j.oregeorev.2014.10.019
0169-1368/

exceptionally large metal reserves. As a consequence the IPB has been, and still is, continuously explored and studied.

Comprehensive studies of the IPB include those of Strauss et al. (1977), Routhier et al. (1978), Barriga (1990), Sáez et al. (1999), Leistel et al. (1998), Carvalho et al. (1999) and Tornos et al. (2000, 2006). Almost all these works are based on structural, petrologic, mineralogical and geochemical studies of the primary mineralization. However, the intense mining activity in the area and the subsequent ore removal, preclude the preservation of supergene ores in the IPB. Therefore, the fact that the Las Cruces deposit has remained buried and preserved by the sedimentary cover provides an excellent opportunity to improve knowledge on the IPB supergene profiles.

In fact, there are very few publications on the IPB supergene profiles. Some deal mainly with the reserves, metallurgy and mining of the gossan cap (García Palomero et al., 1986; Viñals et al., 1995; Sánchez et al., 1996; Roca et al., 1999), while others cover the genesis and evolution of some supergene profiles, such as those of San Miguel (Álvaro and Velasco, 2002), Riotinto (Amorós et al., 1981; Arribas, 1998; Capitán, 2006; Williams, 1950), or Tharsis (Capitán, 2006; Capitán et al., 2003), or provide a general analysis of the IPB gossan (Kosakevitch et al., 1993, 1994; Viallefond, 1994; Velasco et al., 2013).

Regarding the Las Cruces deposit, there are some reports dealing with the genesis and evolution of the cementation zone and gossan. Knigth (2000) suggested a genesis of Las Cruces secondary mineralization in relation to (1) the oxidation of primary sulfides during the last stages of the hydrothermal ore-forming system, and (2) the increasing/decreasing geothermal gradient associated to the tectonic burial and uplifting events affecting the deposits after its genesis. Capitán (2006) proposed for the Las Cruces gossan an evolution controlled by the Miocene transgressive–regressive episodes affecting the area. Blake (2008) and Tornos et al. (2014) suggested that the uncommon mineralogy characterizing the Las Cruces gossan was related to anaerobic microbial activity. Finally, Yesares et al. (2014) described the supergene precious metals mineralizations, suggesting that they were formed by amalgamation of Au and Ag at the gossan bottom.

The present paper represents the first comprehensive study of the Las Cruces deposit as it is based on the geological and structural data obtained at the open pit during the first and second mining phases, on the geochemical interpretation of data from the numerous drill holes conducted by Cobre Las Cruces S.A. during the exploration and evaluation phases, and on the mineralogical studies of the different deposit sectors. All these suggest that the Las Cruces primary massive sulfide deposit is similar to common VMS deposits from the IPB, but the supergene enrichment zone and the gossan exhibit a number of peculiarities that make the Las Cruces deposit noticeably different from other weathering profiles (Blain et al., 1977; Sato, 1960; Scott et al., 2001; Sillitoe, 2005; Taylor, 2011; Thornber, 1985), even from the IPB (Capitán, 2006; Velasco et al., 2013).

This paper includes the first mineralogical and geochemical bulk ore analyses of the Las Cruces deposit as well as the first genetic model that explains the origin of the primary sulfides and the subsequent evolution of the supergene profile.

2. Geological background

2.1. IPB

The IPB is located in the SW corner of the Iberian Peninsula, extending circa 230-km-long and 40-km-wide, from Seville in Spain, to south of Lisbon in Portugal (Fig. 1).

The IPB forms the principal domain of the South Portuguese Zone (Iberian Massif) (Julivert et al., 1974), and is interpreted as a tectono-stratigraphic terrane sutured to the Iberian Massive during Variscan times (Quesada, 1991).

The stratigraphic succession of the IPB consists of Upper Palaeozoic (Middle Devonian–Mississippian) sedimentary and igneous rocks that have been classically subdivided into three lithostratigraphic units: the Devonian Phyllite–Quartzite Group (PQ Group), the Late Devonian–Mississippian Volcano-Sedimentary Complex (VSC) and the Late Visean–Moscovian post-volcanic succession (Culm Group) (Schermerhorn, 1971). The limits of the three units are depositional, although locally they are masked by tectonic.

The PQ Group, dated as Late Givetian to Late Famennian (Van den Boogaard and Schermerhörn, 1975; González et al., 2004), forms the base of the IPB series. It consists of a thick detrital sequence of shales and sandstones representative of a shallow marine platform that evolved at the top in response to basin shallowing (Moreno and Saéz, 1990; Moreno et al., 1996).

The VSC is Late Famennian–Visean in age according to paleontological data (Oliveira, 1990). It is mostly composed of volcanic and subvolcanic rocks interbedded in a detrital sedimentary sequence of shales and volcano-derived sandstones. The VSC is characterized by bimodal volcanism (Mitjavila et al., 1997; Thiéblemont et al., 1998).

Toward the top the VSC gradually evolves into the shaly sequence of the Culm Group (Moreno, 1987; Moreno and Sequeiros, 1989). This unit, Late Visean–Moscovian in age, consists of a thick turbidite sequence of shales and sandstones representing the basin infill in response to tectonic uplift. The Ossa-Morena Zone and the IPB itself have been interpreted as the main source areas (Moreno, 1993).

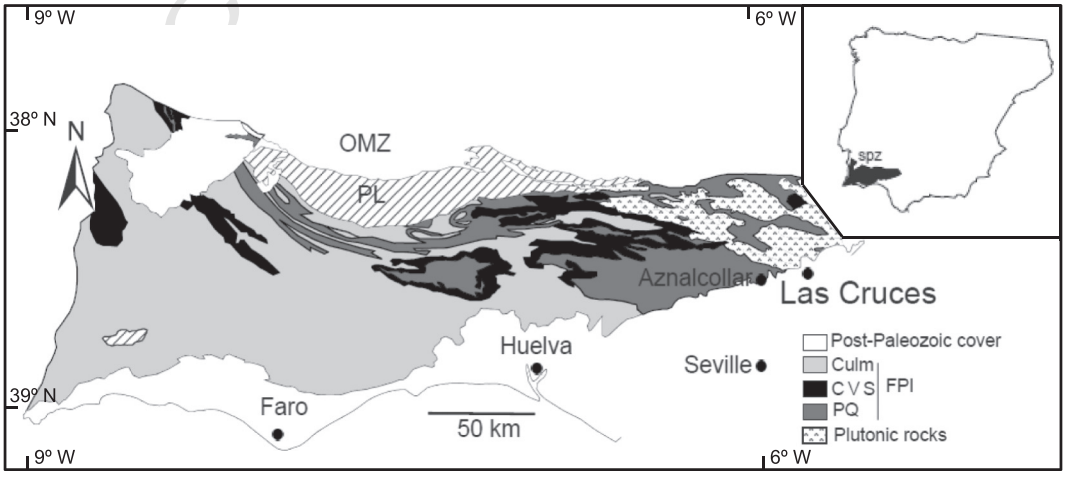

Fig. 1. Geological map of the Iberian Pyrite Belt (modified from Carvalho, 1976), indicating the location of the Las Cruces deposit. Geological abbreviations: IPB, Iberian Pyrite Belt; OMR, Ossa Morena Zone; PL, Pulo do Lobo Terrane.

Please cite this article as: Yesares, L., et al., The Las Cruces deposit, Iberian Pyrite Belt, Spain, Ore Geol. Rev. (2014), http://dx.doi.org/10.1016/j.oregeorev.2014.10.019

Geodynamic interpretations suggest that during Late Devonian–Early Carboniferous the IPB was affected by extensional tectonic processes responsible of the breakdown and segmentation of the basin and the beginning of volcanism (Moreno et al., 1996). This paleogeographic environment favored the massive sulfide deposition (Sáez et al., 1999). The episodic ascent of magma just below the segmented basin could have triggered the establishment of a hydrothermal system. Large volumes of sea water with connate water trapped in the volcanic pile and the Devonian sediments may have been the source of the fluids necessary for the transport and deposition of metals (Sáez et al., 1999; Tornos and Heinrich, 2008).

It is commonly accepted that the massive sulfide deposits in the IPB were deposited between Late Famennian and Early Visean (Nesbit et al., 1999; González et al., 2000; Nieto et al., 2000; Barrie et al., 2002). They occur as lens-shaped stratabound bodies interbedded with black shales and, to a minor extent, with volcaniclastics rocks from the first two felsic volcanic episodes (Barriga, 1990; Routhier et al., 1978), or their stratigraphic equivalents (Aye, 1974; Barriga, 1990; Lécolle and Roger, 1973; Routhier et al., 1978; Ruiz de Almodóvar and Sáez, 1992; Sáez et al., 1999; Strauss and Madel, 1974). Textural analyses show that massive sulfides were formed in different stages (Carvalho and Ferreira, 1993; Leistel et al., 1994; Marcoux et al., 1996) related to the different pulses of the hydrothermal system.

The IPB was intensely deformed during the Variscan orogeny according to a thin-skinned tectonic style (Silva et al., 1990). The Variscan deformation was polyphase, involving three main stages. The first stage, dated as Middle Westphalian (Schermerhorn, 1971; Silva et al., 1990), produced the major regional structures, and was responsible of the thin-skinned deformation, with S-verging asymmetric folds and thrust. The second phase gently folded the main F1 foliation, with vertical, N–S axial planes. Finally, the third deformation stage was related to the late-Variscan fracturing phase, and consisted of two fault systems, an E–W set and a conjugated NNW/SSE and NE/SW system.

The massive sulfide deposits in the IPB are composed mostly of pyrite, with subordinated sphalerite, galena, chalcopyrite, tetrahedrite–tennantite, arsenopyrite, pyrrhotite and many other minor phases as Bi- and Pb-sulfosalts, cassiterite, magnetite, stannite, electrum and cobaltite (García de Miguel, 1990; Marcoux et al., 1996; Sáez et al., 1996 and Sáez et al., 1999; Leistel et al., 1998; Almodóvar et al., 1998).

2.2. Post-Variscan Sedimentary cover

Due to the Tertiary marine transgression, the south and western margins of the IPB were buried by Neogene-Quaternary sediments of the Guadalquivir and Sado Basins (Strauss and Madel, 1974). The Neogene infill of the Guadalquivir Basin is comprised mostly by a carbonate and detrital sequence that unconformably overlies the Palaeozoic basement (González-Delgado et al., 2004; Sierro et al., 1990). In Las Cruces area this is circa 150-m-thick, but to the south it thickens to as much as 1.5 km around Seville (Sala, 1984). This sequence is divided in two main formations in the Las Cruces area. At the base, the Niebla Formation consists of a calcarenite series overlaying a basal conglomerate. This unit, of continental to shallow marine origin, has a thickness range of 5–15 m, and is gently wedging to the south. Conformably over this unit the marine Arcillas de Gibraleón Formation comprises a 100–150-m-thick sequence of semi-consolidates glauconitic sands interbedded with marls and silts. The basal conglomerate, calcarenites and glauconitic sands, jointly with the upper part of the Palaeozoic weathering cap constitute the "Niebla-Posadas" aquifer.

3. Samples and analytical procedures

The observations and geological/structural interpretations presented in this paper were made during the first and second mining stage at Las Cruces open pit. The 3D cartography was made in collaboration with the Technical Department of Cobre Las Cruces S.A., with the help of a Total Station (LEICA-TCRA 1203). Cartography digitalization was made with the software packages AutoCAD 2009 and ArcGIS 9.3.

Sampling was undertaken also during the first and second mining stages, although additional samples were collected from drill holes and blast holes conducted by Cobre Las Cruces S.A. during the exploration, production and evaluation stages. The mineralogical analysis was done by transmitted and reflected light microscopy (microscope Nikon eclipse lv100pol), X-ray Diffraction (XRD) (model Broker D8 Advance) and Scanning Electron Microscopy-Energy Dispersive Spectroscopy (SEM-EDS) (model JMS-5410 equipped with a microanalyzer Link Oxford). All these equipments were located at the University of Huelva.

The geochemical zonation and the vertical distribution of the Las Cruces deposit were examined after the statistical treatment of the Las Cruces analytical database. This database includes geochemical analyses from 305 drill holes conducted during the exploration and evaluation phases. Pb, Zn, Cu, Bi, Ag, Hg, Au, Fe and S content was measured in 9832 selected samples from the primary sulfides, the Cu-rich cementation zone and the gossan. The chemical assays were undertaken in several full-accredited laboratories. A first set of samples (drill holes numbers CR001–CR256) was measured by Anamet Services (Avonmouth, UK), a second set of analyses (drill holes numbers CR257–CR301) was carried out at OMAC Laboratories (Ireland), and a last set of samples was determined at AGQ Labs (Seville, Spain). All analyses have been conducted by the same methodology. Pb, Zn, Cu, Bi, Ag, Hg and Fe were determined after 4 acid digestions (HF, HNO_3, HCl and $HClO_4$) with Inductively Coupled Plasma-Optical Emission Spectrometry (ICP-OES). Total S concentration was carried out by Leco, and Au form the selected samples were performed by Ni fire assay followed by atomic absorption spectroscopy (AAS).

4. Geology of the Las Cruces deposit

The Las Cruces ore deposit is located in the south eastern corner of the IPB. It is a typical VMS deposit associated to the first felsic volcanic episode of the IPB. U–Pb isotope dating from altered dacite tuffs below the massive sulfide deposit gives an age of 353.97 ± 0.69 Ma (Barrie et al., 2002).

4.1. Ore stratigraphy

The Las Cruces deposit is a massive sulfide body, averaging 60-m-thick and reaching 100-m-thick, interbedded in a thick sequence of black shales and felsic volcanic and volcaniclastic rocks.

The footwall sequence exceeds 350-m-thick, and is dominated by highly deformed felsic volcaniclastics interbedded with black shales that become increasingly the dominant lithology to the west (Knigth, 2000). This sequence includes a stockwork type mineralization cross-cutting the footwall rocks. Chloritic and quartz–sericitic are the main hydrothermal alterations.

The hanging wall consists predominantly of black shales interbedded with subordinate volcaniclastics. Extensive zones of brecciation are also present. There, clasts with alteration rims of different thickness are held by a fine chlorite–quartz–sericite matrix (Knigth, 2000).

4.2. Structure of the Las Cruces deposit

The absence of natural outcrops of the Variscan basement in the vicinity of the Las Cruces deposit makes difficult the analysis of its tectonic structure. Data from the open pit and drill holes suggest the stacking of tectonic slices as the main structural feature of the Las Cruces deposit. Detachment is often produced along the black shale hosting horizons. This tectonic style is in agreement with the thin-skinned model proposed for the whole IPB (Silva et al., 1990). This model has been also reported for the neighboring Aznalcóllar district (Almodóvar

Please cite this article as: Yesares, L., et al., The Las Cruces deposit, Iberian Pyrite Belt, Spain, Ore Geol. Rev. (2014), http://dx.doi.org/10.1016/j.oregeorev.2014.10.019

et al., 1998). Late Variscan faults produced minor modification of the general structure of the deposit, but played an important role in the metal distribution during the secondary enrichment stage. Two fault systems are observed in the area (Figs. 2, 3, 4a, b, c and d). The older one includes NNW/SSE trending faults and is intersected by the younger system, formed by E–W high angle faults. Both late Variscan fault systems were reactivated during the Alpine cycle.

4.3. Deposit morphology and ore facies

The Las Cruces ore deposit shows a complex shape as a result of the Variscan deformation and the subsequent weathering during post-Variscan exhumation (Fig. 2). As discussed above, the general architecture of the deposit is composed by three different ore facies: primary sulfides, including massive, semi-massive and stockwork type mineralization, secondary enrichment zone and gossan (Figs. 2, 4a, b, c, d, 5a, b, c and d).

The primary massive sulfide body has been preserved mainly in the northern flank and, in a minor proportion, in the hinge of Variscan fold (Fig. 2). It has an average thickness of about 60 m and extends over 1 km in E/W direction, deeping 35° to the north. This northern extension has been recognized by exploratory drill up to 600 m deep and remains still open downwards (Knigth, 2000).

The primary deposit consists of a polymetallic massive and semi-massive body and a Cu-rich pyritic stockwork. It is formed mainly of pyrite together with subordinate amounts of chalcopyrite, sphalerite and galena. Tetrahedrite–tennantite, arsenopyrite and several Bi and Pb-sulfosalts are often present as accessory minerals. As occurs in other IPB deposits, the ore is typically medium-fine grained, with very diverse textural relationships. Primary sulfide includes a well-developed stockwork below the massive sulfide deposit (Fig. 2). This is very irregular in shape and mineralogy, including barren pyrite, polymetallic and copper-rich facies.

The cementation zone represents the supergene copper enrichment zone of primary sulfides from massive ore and stockwork. It

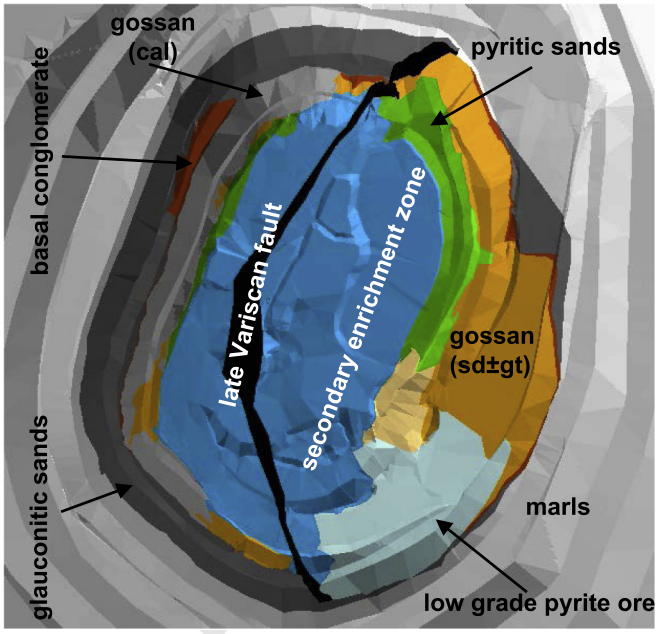

Fig. 3. Graphic projection of the first phase to the Las Cruces open pit. Abbreviations: cal: calcite; gt: goethite; and sd: siderite.

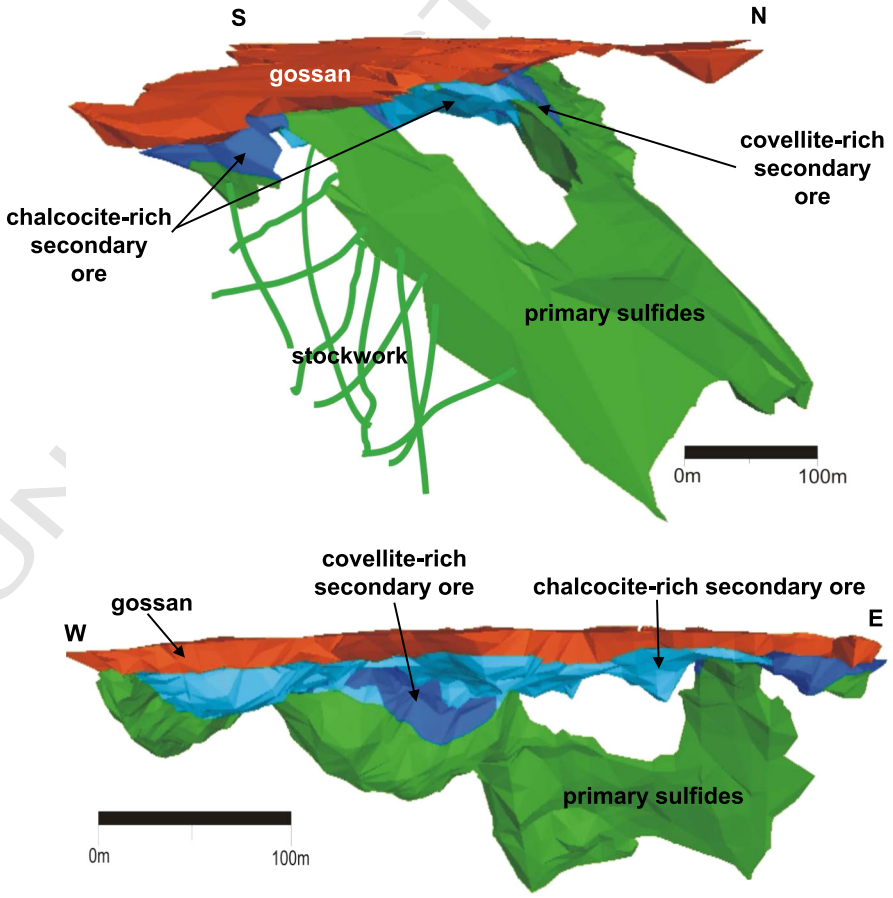

Fig. 2. 3D model to the Las Cruces deposit.

Please cite this article as: Yesares, L., et al., The Las Cruces deposit, Iberian Pyrite Belt, Spain, Ore Geol. Rev. (2014), http://dx.doi.org/10.1016/j.oregeorev.2014.10.019

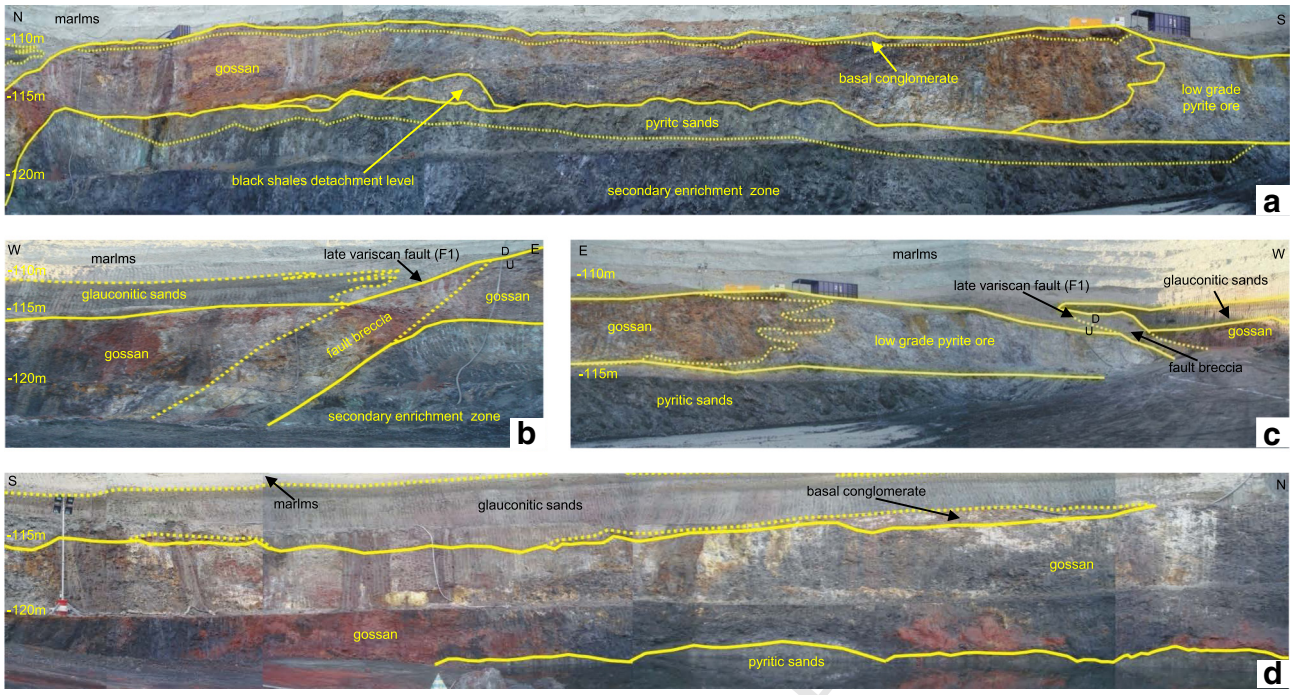

Fig. 4. Views of the first phase of the Las Cruces open pit. a) and (d) east and west faces showing gossan in sharp contact with massive sulfides; b) and c) north and south faces showing gossan and massive sulfides cutting by a late Variscan fracture, and overlain by sedimentary cover.

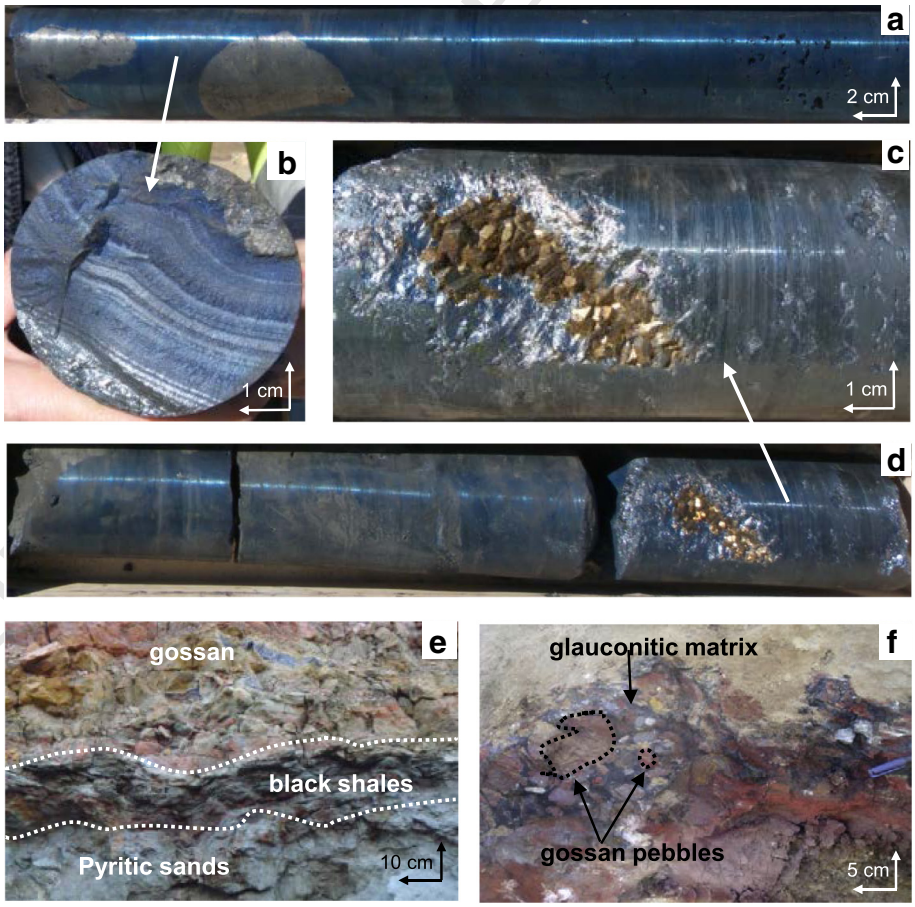

Fig. 5. Representative images of selected drill cores and outcrops. a) covellite-rich secondary mineralization replacing primary pyrite; b) banded texture in covellite-rich secondary ore; c) and d) oxidized euhedral crystals of djurleite in chalcocite matrix; e) sheared black shale level which separates gossan and decomposed barren pyrite at the top of the secondary enrichment zone; f) basal conglomerated including gossan pebbles in a glauconitic sand matrix.

Please cite this article as: Yesares, L., et al., The Las Cruces deposit, Iberian Pyrite Belt, Spain, Ore Geol. Rev. (2014), http://dx.doi.org/10.1016/j.oregeorev.2014.10.019

preferentially develops through highly permeable zones associated to fractures (Fig. 3). Subvertical faults generated during the late Variscan deformation exert the main control on the distribution of the secondary mineralization (Fig. 4). This is the reason why the cementation zone has an irregular, non-tabular shape overlying the primary sulfides (Figs. 2, 3, 4a, b, c and d), as it was preferentially developed irregularly through these faults up to very deep levels (Fig. 4).

The cementation zone was formed beneath the gossan and exhibits an essentially flat top and an irregular base (Fig. 2). The Cu-rich secondary mineralization consists of a 50-m-thick lens. In addition, the secondary Cu-rich mineralization is also developed as a 12-m-thick lens located within the primary sulfides (Fig. 2). This second lens is associated to a deeper subhorizontal fault zone. Both Cu-rich secondary lenses are connected by subvertical late Variscan faults.

Mineralogical and textural features of the secondary sulfides reflect the nature of the primary mineralization and the degree of supergene alteration. The Cu-assemblage in the principal Cu-rich secondary lens consists mainly of chalcocite, digenite, djurleite, covellite, bornite and enargite, together with subordinate amounts of chalcopyrite and tetrahedrite–tennantite. Pyrite, sphalerite and galena are the main gangue minerals. The deepest lens of secondary Cu enrichment within the primary sulfides is dominated by covellite, with pyrite as the main gangue mineral.

A crumbled pyrite lens is located between the gossan and the Cu-rich secondary mineralization. It is constituted by a 0-to-5-m-thick of sand-like granular pyrite which is part of the leaching profile (Figs. 3 and 4).

The gossan mineralization is located between the upper secondary enrichment zone and the Tertiary sedimentary cover. Its thickness ranges from 0-to-20-m, being thicker at the central and western parts of the deposit, and appearing gradually eroded eastward (Figs. 2, 3, 4a, b, c and d). The gossan profile shows an unusual mineralogy, mostly comprised of newly-formed siderite, calcite, Fe-sulfides and galena and relicts of goethite and hematite (as explained below).

Two different types of contacts have been developed between the gossan and the sulfides. In areas dominated by vertical faults the contact with the cementation zone is transitional, but in the remaining areas, the base of the gossan has a sharp contact with the cementation zone (Figs. 3, 4a, b). Within these areas the gossan includes at the base a thin level of black shales (5–15-cm-thick) intensely deformed (Fig. 5e). According to the kinematic markers observed, these black shales acted as a detachment horizon for the thrusts of the main Variscan deformation phase.

The stratigraphic contact between the gossan and the hanging wall Cenozoic series is marked by an erosional and angular discordance (Figs. 3, 4b, c and d). The occurrence of gossan pebbles within the basal conglomerate level of the Tertiary series (Fig. 5f) indicates that weathering and oxidation of the massive sulfides predate the transgressive Tortonian deposits (Moreno et al., 2002).

5. Mineral assemblages

5.1. Primary ore

The mineralogical features of the Las Cruces primary sulfides are similar to other IPB massive sulfides deposits (García de Miguel, 1990; Marcoux et al., 1996). Pyrite is the most abundant phase, while sphalerite, galena, chalcopyrite, tetrahedrite–tennantite and arsenopyrite are common, and Bi and Pb-sulfosalt subordinate phases. A synoptic overview of primary ores, mineral associations and texture relationships is outlined in Table 1, Fig. 6 and described further below.

Three facies have been identified.

- *Pyrite-rich facies*
  This facies constitutes the bulk of the massive sulfide body. It consists mainly of pyrite and minor galena, sphalerite, chalcopyrite and tetrahedrite–tennantite. Pyrite shows a textural evolution from framboidal and collophorm to euhedral crystals, often fractured (Table 1 and Fig. 7a, b). Galena and sphalerite are common as filling void whereas chalcopyrite and tetrahedrite–tennantite usually occur as veinlets or replacing pyrite crystals.
- *Polymetallic facies*
  It is characterized by pyrite, sphalerite and galena, with minor chalcopyrite, tennantite–tetrahedrite, arsenopyrite and Pb–Sb–sulfosalts (Fig. 7c and d). This mineral association typically shows a banded pattern of massive pyrite, sphalerite, galena and chalcopyrite. The textural relationships between these sulfides are shown in Table 1.
- *Cu-rich facies*
  It is mainly formed of pyrite and chalcopyrite, including sphalerite, galena, arsenopyrite, tetrahedrite–tennantite and Bi-minerals as subordinated minerals (Fig. 7e and f). This is the most common mineral association in the stockwork type mineralization and, locally, as late-fracture filling in primary massive sulfides. Textural relationships between pyrite, chalcopyrite and the other sulfides are shown in Table 1.

5.2. Secondary copper ore

The Cu-rich secondary mineralization at Las Cruces occurs as replacement bodies on massive sulfide and stockwork type mineralizations. The cementation zone mostly includes Cu-rich sulfides such as chalcocite and covellite, with bornite and enargite as main subordinate phases. Remnants of primary chalcopyrite and tetrahedrite–tennantite are also common.

Within the Cu-rich secondary mineralization, three main mineral associations, with distinctive mineralogical and textural patterns, have been identified (Table 2 and Fig. 6).

- *Association I*
  This association is formed by remnants of primary Cu–Fe-sulfides and by an early generation of secondary Cu-sulfides (Fig. 8a, b).
  The primary mineralization relicts consist mainly of pyrite, chalcopyrite, tetrahedrite–tennantite, and minor sphalerite and galena. The supergene Cu-sulfides assemblage includes chalcocite, digenite, djurleite, covellite, enargite and bornite. Both primary and secondary sulfide assemblages show evidences of alteration. Their textural relationships consist mainly of dissolution-replacement patterns (Table 2).
  Four crystallization sequences relating both assemblages have been identified: (i) Chalcopyrite → bornite → chalcocite + covellite; (ii) Tetrahedrite–tennantite → enargite → chalcocite + covellite; (iii) Chalcopyrite → chalcocite; and (iv) Tetrahedrite–tennantite → chalcocite.
- *Association II*
  It comprises of Cu-sulfides of the chalcocite group filling voids and micro-fissures of the primary pyrite (Fig. 8c). Pyrite grains exhibit the primary textures described above (Table 2), although dominated by cataclastic textures. Pyrite clasts are angular to slightly rounded, and are enclosed by massive chalcocite and digenite.
  These two mineral assemblages feature different grain contacts. Pyrite and secondary Cu-sulfides usually show sharp contacts without evidences of corrosion. Chalcocite and digenite generally occur as rims along pyrite grain boundaries and filling fractures. Locally, the contact between pyrite and Cu-sulfides is more complex. In such cases, pyrite shows evidences of alteration including corrosion embayments and evidence of dissolution/precipitation involving the replacement of pyrite by chalcocite along pyrite grain margins. In addition, chalcocite and digenite usually show intergrowths with minor covellite patches and skeletal aggregates of galena.
- *Association III*
  It includes relicts of the first generation of supergene Cu-sulfides described in the associations I and II, together with overgrowths of a

Please cite this article as: Yesares, L., et al., The Las Cruces deposit, Iberian Pyrite Belt, Spain, Ore Geol. Rev. (2014), http://dx.doi.org/10.1016/j.oregeorev.2014.10.019

Table 1
Mineralogical patterns of Las Cruces primary mineralization.

Mineral association	Mineralogy	Texture	Example
Pyrite-rich facies	py, (gn, sl, cp, td–tt)	*py:* massive; framboidal; colloform; banded; euhedral; replacement; recrystallization. *gn, sl, cp, td–tt:* disseminations; veinlets; filling voids; banded, recrystallization, overgrowth.	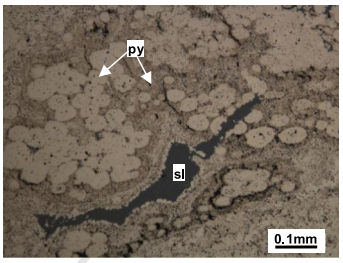
Polymetallic facies	py, sl, gn, (cp, td–tt, apy, Pb–Sb-sulfosalts)	*py:* massive; colloform; euhedral; granoblastic; replacement with polymetallic sulfides. *sl, gn, cp, td–tt, apy, Pb–Sb-sulfosalts:* massive; disseminations; banded; filling voids; intergrowth; fracture sealing on cataclastic py; euhedral crystals; sl with cp disease.	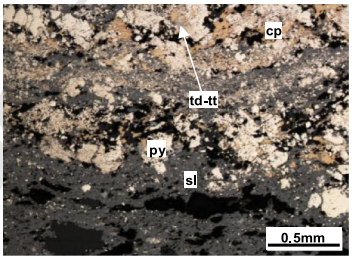
Cu-rich facies	py, cp, (sl, gn, td–tt, Bi-sulfides, apy)	*py:* massive; euhedral; cataclastic. *cp:* massive; disseminations; filling interstices; euhedral and subeuhedral crystals; overgrowth; late-fracture filling. *sl, gn, cp, td–tt, apy, Bi-sulfides:* disseminations; filling voids; intergrowth; fracture sealing on cataclastic py; sl with cp disease.	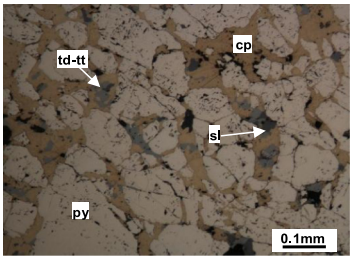

Mineral abbreviations: py—pyrite; gn—galena; sl—sphalerite; cp—chalcopyrite; td—tetrahedrite; tt—tennantite; apy—arsenopyrite.

new generation of supergene Cu-sulfides associated with newly-formed calcite, pyrite and galena (Fig. 8d, e, f, g).

The relicts of secondary Cu-sulfides I comprise mainly of covellite and chalcocite. This assemblage exhibits different textural features, as shown in Table 2. The assemblage of supergene Cu-sulfides II consist of minerals of chalcocite group including chalcocite and djurleite. The main textural features are shown in Table 2.

The textural relationship between Cu-sulfides II and supergene calcite is complex. Both phases generally appear either as intergrowths or filling fractures and intergranular open spaces. Nevertheless, occasionally calcite occur filling fractures associated with Cu-sulfides II. In such cases, calcite seems to be somewhat later than Cu-sulfides, and occurs as overgrowths on minerals of the chalcocite group.

Two recrystallization sequences are observed: (i) covellite I → chalcocite–djurleite II + calcite ± galena ± pyrite; and (ii) chalcocite I → djurleite II + calcite ± galena ± pyrite.

The association III locally includes Ag-sulfides and Ag-sulfosalts such as proustite, pyrargirite, myargirite, acantithe and stembergite. These Ag-rich minerals are located in fault brecciated bands within the massive sulfide body (Fig. 8 h).

5.3. Gossan

The mineralogical and textural features that define and differentiate the Las Cruces gossan from other weathering profiles in the IPB are detailed by Yesares et al. (2014). They can be summarized as follow:

- The high mineralogical heterogeneity, both vertically and laterally, thus preventing the development of well-defined horizons, typical in these type of weathering profiles (Scott et al., 2001), even within the IPB (Capitán, 2006; Velasco et al., 2013).
- Fe-oxides, oxyhydroxides and sulfates occur in the Las Cruces gossan, but unlike other gossans, not as major minerals. Paradoxically, the major minerals are siderite, Fe-sulfides and galena, instead Fe-oxihydroxides.
- Precious metals of the gossan occur mainly concentrated toward to the bottom, amalgamated with Hg (Yesares et al., 2014).

Mineralogical and textural features highlight three main mineral associations in the Las Cruces gossan, as summarized in Table 3 and Fig. 6.

- *Association I*
  This association is formed by a first generation of goethite and hematite. Both minerals mainly exhibit massive textures (Table 3), and appear locally as isolated fragments in the weathering profile. Oxyhydroxide fragments are slightly rounded and show evidence of corrosion. Relicts of Fe-oxyhydroxides are enclosed within a cement of microcrystalline siderite (Fig. 9a).
- *Association II*
  It consists of a second generation of Fe-oxyhydroxides and the first generation of siderite (Fig. 9b, c). Common textures for this mineral association are shown in Table 3. These minerals usually fill fractures and open spaces along the weathering profile, although frequently, these fractures and open spaces appear only filled by siderite. In such cases, siderite exhibits several different textural features as shown in Table 3.
- *Association III*
  It is characterized by a second generation of siderite associated with secondary sulfides as galena, marcasite, pyrite, greigite and pyrrhotite (Fig. 9d, e, f). This mineral association is observed filling fractures and open spaces all along the weathering profile. Siderite II and sulfides show complex textures and relationships, as indicated in Table 3. This mineral association is also present at the gossan

Please cite this article as: Yesares, L., et al., The Las Cruces deposit, Iberian Pyrite Belt, Spain, Ore Geol. Rev. (2014), http://dx.doi.org/10.1016/j.oregeorev.2014.10.019

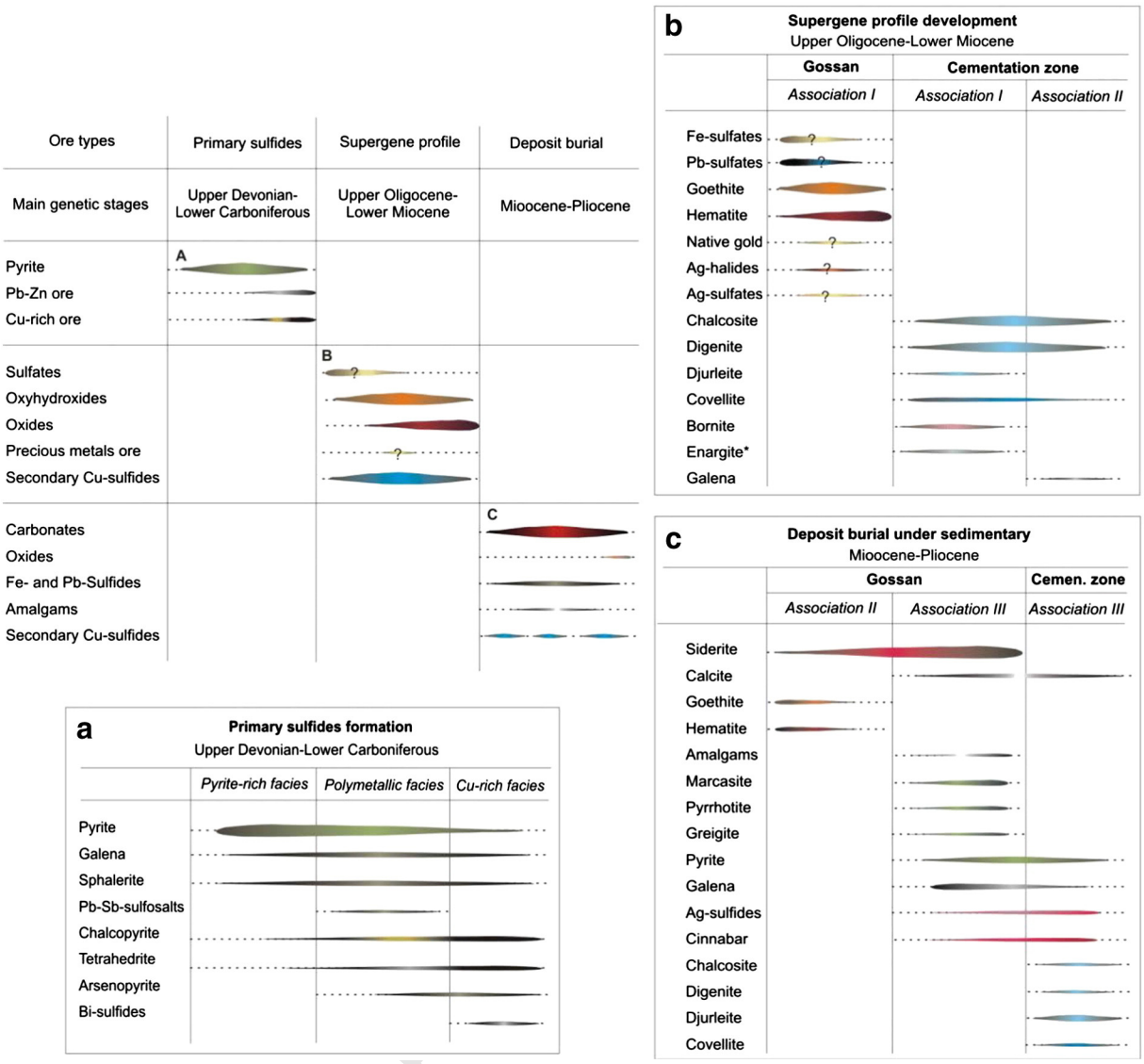

Fig. 6. Mineral association sequence of the Las Cruces deposit ore types.

footwall, where galena and Fe-sulfides occur associated with Ag-sulfides, Ag-sulfosalts, cinnabar and Ag–Au–Hg amalgams (Fig. 9f).

6. Metal associations, zoning and distribution

The geochemical data obtained during the exploration and exploitation stages shows significant differences in the distribution of major and minor elements within the Las Cruces deposit. This, together with the ore type distribution and the mineralogical composition, points to a complex internal structure.

– *Primary mineralization*

Primary sulfides show a rough zonation in terms of base metal and Fe (Figs. 10, 11 and 12). Fe content is fairly constant in the primary mineralization (Figs. 11 and 12), while the distribution of base metals permits the identification of the three ore types described above, i.e., pyritic, Cu-rich and polymetallic ores (Figs. 10, 11 and 12). Pb and Zn are concentrated mainly in the polymetallic mineralization, with average values of 2 wt.% and 4.5 wt.%, and maximum values of 27 wt.% and 27.5 wt.%, respectively (Table 4). Bivariant diagrams for these elements denote positive correlation, although with an important data dispersion (Fig. 10a).

Cu concentrates mostly in the Cu-rich mineralization, with average and maximum values of 4 wt.%, and 19 wt.%, respectively (Table 4). According to the bivariant diagrams, Cu from the primary sulfides does not correlate with any other base metal (Fig. 10b and c). In this kind of mineralizations, Cu correlates more significantly with Bi, although displaying high data dispersion (Fig. 10d).

The polymetallic mineralization shows Ag–Pb and Hg–Zn positive correlations, but with high data dispersion (Fig. 10e and f). Ag also correlates positively with Cu in the Cu-rich mineralization (Fig. 10 g), but nevertheless Cu lacks positive correlation with Hg (Fig. 10 h). Ag and Hg concentrate principally in the polymetallic mineralization. Ag shows average and maximum values of 42.5 ppm and 713 ppm, respectively (Table 4), and Hg reaches anomalous maximum values of 814 ppm, with an average of 52 ppm (Table 4).

Au also concentrates mainly in the polymetallic mineralization, with average and maximum values of 0.7 ppm and 8.4 ppm, respectively (Table 4). According to the bivariant and vertical distribution diagrams, Au shows a clear positive correlation with Cu, Bi and Ag (Fig. 10i, j and k) in the polymetallic facies, and a positive correlation with As (Fig. 10 l) in all the primary mineralizations.

The geochemical zonation, as well as the vertical evolution of base metals in the primary mineralization of the Las Cruces ore deposit,

Please cite this article as: Yesares, L., et al., The Las Cruces deposit, Iberian Pyrite Belt, Spain, Ore Geol. Rev. (2014), http://dx.doi.org/10.1016/j.oregeorev.2014.10.019

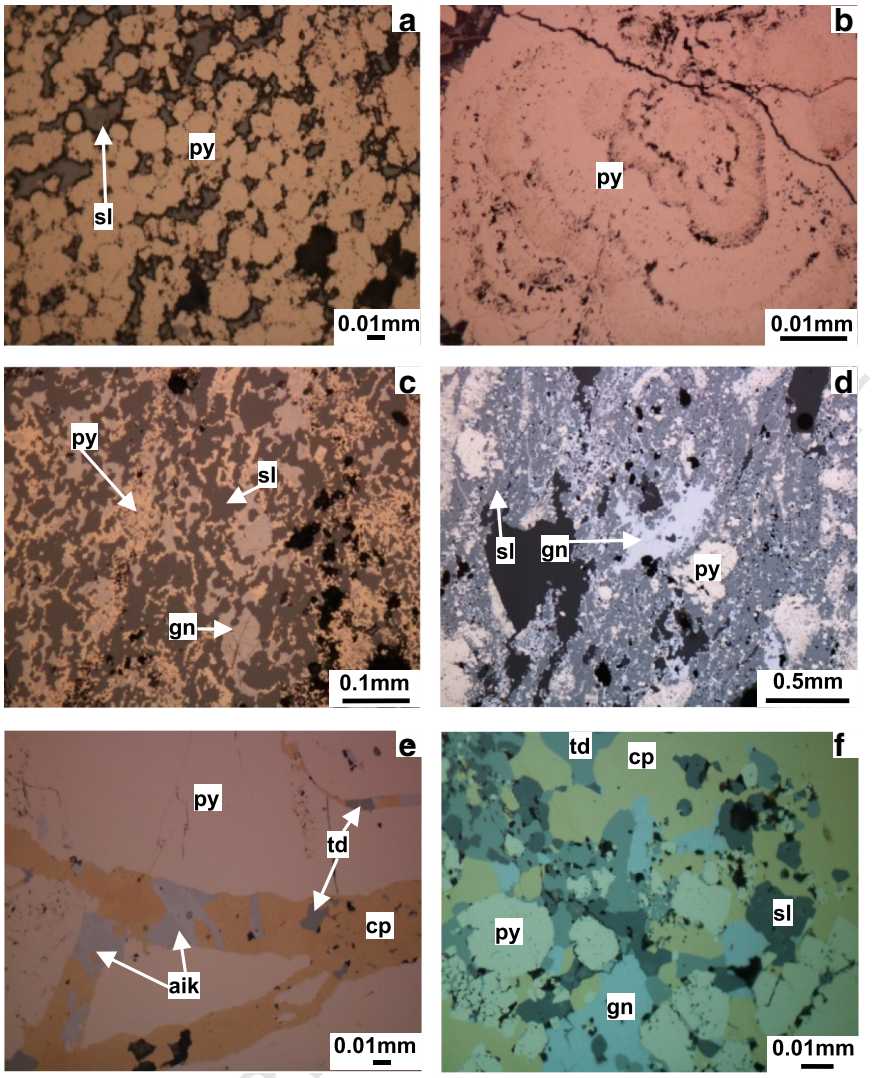

Fig. 7. Reflected light microscopy images of the Las Cruces primary ore. a) *pyritic facies* comprised of framboidal pyrite (py) with intergranular sphalerite (sl); b) *pyritic facies* formed by colloform pyrite; c) and d) *polymetallic facies* composed by pyrite (py) and interstitial sphalerite (sl) and galena (gn); e) *Cu-rich facies* comprised of scattered chalcopyrite (cp) filling open spaces in pyrite (py), intergrowth with tetrahedrite (td) and Bi-minerals as a aikinite (aik); f) *Cu-rich facies* formed by pyrite (py) and an intergrowth between chalcopyrite (cp), sphalerite (sl), tetrahedrite (td) and galena (gn).

agrees with the mineralogical associations described here. The constant values of Fe, the high correlation of this with S (Figs. 11 and 12), and the mineralogical analyses, support the fact that pyrite is the major mineral phase in the primary mineralizations (Fig. 7). Pb and Zn are mainly associated with galena and sphalerite, respectively, in the polymetallic mineralization (Fig. 7c and d). Cu concentrates in the Cu-rich mineralization as chalcopyrite, tetrahedrite–tennantite, and Cu–Bi-sulfosalts (Fig. 7e and f).

Hg is systematically associated with the polymetallic mineralization. SEM-EDS analysis suggests that Hg in the primary mineralization of the Las Cruces deposit occurs within sphalerite and minerals of the tetrahedrite group, all constituting major phases in the polymetallic mineralization. Ag and Au occur as well as in the polymetallic and Cu-rich mineralizations. According to the SEM-EDS analysis Ag is associated with minerals of the tetrahedrite group, while Au is probably included within the arsenopyrite lattice, in the polymetallic and Cu-rich mineralizations (Yesares et al., 2014).

– *Supergene profile*

Vertical distribution diagrams generally show constant values of Fe, both in the primary sulfides and supergene enrichment zone (Fig. 11 y 12). The average Fe concentration in the gossan profile is about of 15 wt.%, lower than those for the primary sulfides and cementation zone (Fig. 11 y 12).

Vertical distribution diagrams also show that the cementation zone is depleted in Pb and Bi (Figs. 11 and 12), with Pb and Bi average values of 0.7 wt.% (Table 4) and 10 ppm (Figs. 11 and 12), respectively. By contrast, the gossan exhibits a noticeable enrichment in Pb and Bi, with average values of 2.7 wt.% and 315 ppm respectively (Table 4, Figs. 11 and 12).

As occurs in other similar deposits, the gossan is impoverished in Cu. This significantly concentrates in the cementation zone (Figs. 11 and 12), reaching values up to 39.5 wt.% Cu (Table 4). The supergene Cu-rich mineralization shows a complex structure based on the Cu distribution. Such distribution has enabled the identification of the two bodies within the cementation zone described above (Fig. 12).

Ag and Hg have an apparent contradictory behavior in the supergene profile. Bivariant diagrams do not display positive correlation between these two elements, neither in the gossan (Fig. 13) nor in the cementation zone (Fig. 14). However, the vertical distribution diagrams show a noticeable parallelism between the absolute values of both elements in these two zones (Figs. 11 and 12). Also noticeable is the fact that the supergene profile is enriched in Ag and Hg

Please cite this article as: Yesares, L., et al., The Las Cruces deposit, Iberian Pyrite Belt, Spain, Ore Geol. Rev. (2014), http://dx.doi.org/10.1016/j.oregeorev.2014.10.019

Table 2
Mineralogical patterns of Las Cruces Cu-rich secondary mineralization.

Mineral association	Mineralogy		Texture		Example
	Relict	New-formed	Relict	New-formed	
Association I	py, cp, td–tt (gn, sl)	cc I, (dg I, cv I, fam I-eng I, bn I)	*py:* massive; framboids, colloforms; euhedral and anhedral crystals, corrosion gulfs. *cp, td–tt:* intergrowth, overgrowth; filling voids and fractures; corrosion gulfs.	*cc I, dg I, cv I, fam I-eng I, bn I:* massive; intergrowths; overgrowths; lamellae; patches; rims; recrystallization; replacement; colloforms; granular aggregates; veinlets.	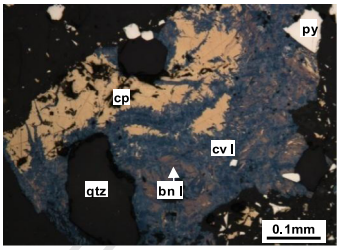
Association II	py	cc I, (dg I, cv I)	*py:* massive; framboids, colloforms; euhedral aggregates; cataclastic shattering; corrosion gulfs.	*cc I, dg I, cv I:* massive; filling fractures; rims; intergrowth; overgrowths; patches; veinlets.	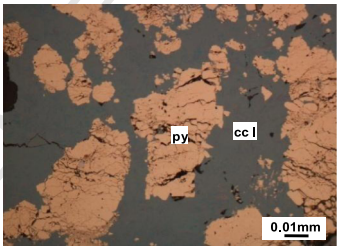
Association III	py, cc I, (dg I, cv I)	dj II, cc II, cv II, (cal, gn II, py II, Ag-sulfides)	*py:* massive; cataclastic. *cc I, cv I, dg I:* massive; intergrowths; euhedral aggregates; corrosion gulfs; veinlets.	*dj II, cc II, dg II and cv II:* euhedral aggregates of coarse grain size; veinlets; intergrowths; overgrowth; patches; rims. *cal and dj II* intergrowth; overgrowth; filling of fractures and voids. *gn, py:* skeletal aggregates.	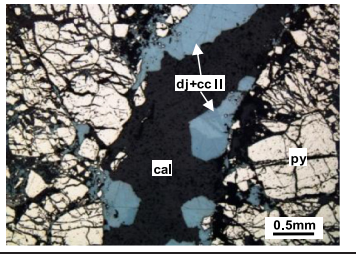

Mineral abbreviations: py—pyrite; gn—galena; sl—sphalerite; cp—chalcopyrite; td—tetrahedrite; tt—tennantite; cc—chalcosite; cv—covellite; dg—digenite; dj—djurleite; fam—famatinite; eng—enrgite; bn—bornite; cal—calcite.

with regard the primary mineralization. Ag and Hg average values of the cementation zone are respectively 27 ppm and 25 ppm, reaching extreme values up to 1472 ppm y 11,085 ppm (Table 4). Close to the contact between the gossan and the cementation zone, Ag and Hg clearly concentrate and better correlations between these two elements can be observed (Figs. 11 and 12), showing average values of 165.5 ppm y 155 ppm, and maximum values of 18,950 ppm and 10,500 ppm, respectively (Table 4).

According to the bivariant (Fig. 14) and vertical distribution diagrams (Figs. 13 and 14), Au content of the cementation zone is similar to the primary mineralizations. Besides, correlations between Au with other elements are limited. In the gossan, the bivariant diagrams do not show relevant correlation of Au with other elements (Fig. 13), but the vertical distribution diagrams display, by contrast, an important enrichment of Au to the base of the gossan (Figs. 11 and 12), with values up to 353 ppm (Fig. 11 and Table 4). In addition, this element exhibits a high correlation with Ag and Hg (Figs. 11 and 12).

Fe is mainly associated with siderite, goethite, hematite and Fe-sulfides in the gossan (Fig. 9), and with primary and/or newly-formed pyrite in the cementation zone (Fig. 10).

– Pb is associated with galena through the entire supergene profile, occurring more abundantly in the gossan as newly-formed mineral (Fig. 9e), thus justifying the high Pb content in this zone.

In the cementation zone, Cu is generally associated with supergene Cu-sulfides (Fig. 8), but in the gossan, Cu minerals are absent. This confirms the typical impoverishment of Cu in this part of the profile. Ag and Hg concentrate in the cementation zone as Ag-sulfides and sulfosalts and as cinnabar respectively (Fig. 8 h). The high grades of Au, Ag and Hg in the gossan, especially toward its base, are explained mineralogically with the abundance of Ag-sulfides and sulfosalts, and amalgams of Au–Ag–Hg and Ag–Hg (Fig. 9f).

7. Discussion

7.1. Comparison with other VMS deposits

In general terms, the Las Cruces primary mineralization is similar to other VMS deposits (Franklin et al., 1981, 2005; Hannington and Scott, 1989; Herzig and Hannington, 1995), showing also analogies with most of the VMS deposit in the IPB (Leistel et al., 1998; Saéz et al., 1996; Sáez et al., 1999; Tornos, 2006 and Tornos et al., 2000). The Q21 major similarities between the primary sulfides of Las Cruces and other IPB deposits are:

(i) *Morphology.* As most of the IPB deposits, the Las Cruces massive sulfide body occurs as a tabular lens concordant with the stratification and underlain by a cone-shaped stockwork (Fig. 2);

(ii) *Size and tonnage.* Size of IPB deposits is highly variable, ranging between few-meters-thick and <4 Mt (e.g. Lagoa Salgada; Oliveira et al., 2011), and 100-m-thick, 1.5-km-long and >500 Mt Q22 (e.g. Riotinto; Almodóvar et al., 1997). The Las Cruces deposit, with 60–100-m-thick, 1-km-long and 42 Mt, is therefore a medium-sized body;

(iii) *Host rocks.* The Las Cruces orebody is mainly hosted by sedimentary rocks including black shales and felsic volcaniclastic rocks. The IPB deposits are generally hosted by black shales, coherent felsic volcanics and related volcaniclastic rocks (e.g. Massa Valverde; Ruiz et al., 2002, Sotiel-Migollas; Tornos, 2006 and Q23 Neves Corvo; Relvas et al., 2001), and minor mafic rocks

Please cite this article as: Yesares, L., et al., The Las Cruces deposit, Iberian Pyrite Belt, Spain, Ore Geol. Rev. (2014), http://dx.doi.org/10.1016/j.oregeorev.2014.10.019

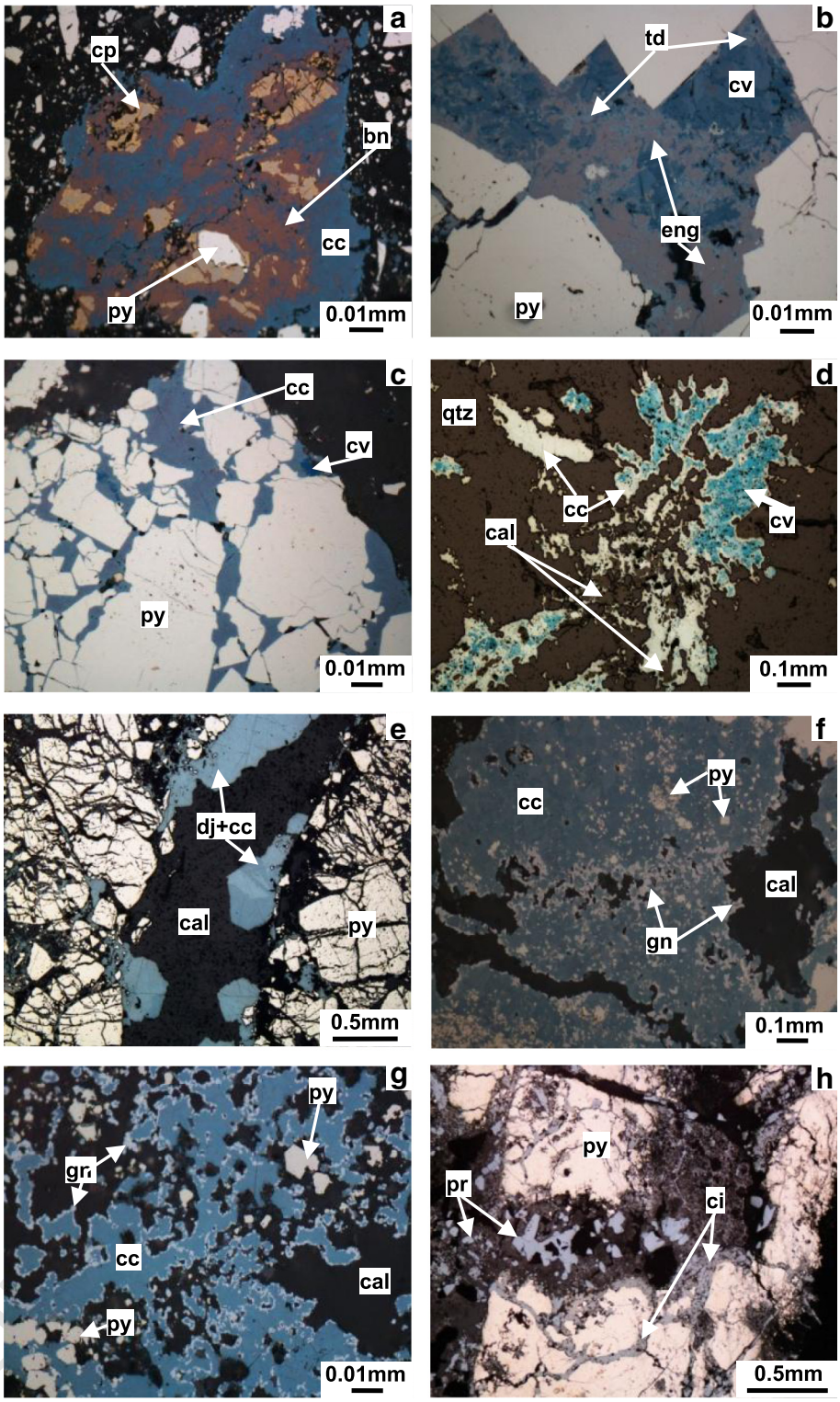

Fig. 8. Reflected light microscopy images of the Las Cruces secondary sulfide ore. a) *association I* composed by chalcopyrite (cp) relicts replaced by bornite (bn) and chalcocite (cc); b) *association I* formed by pyrite (py) with tetrahedrite (td) filling interstices. Tetrahedrite is replaced by enargite (eng) and covellite (cv); c) *association II* comprised of chalcocite (cc) with covellite (cv) patch infilling fractures in massive pyrite (py); d) *association III* formed by covellite (cv) filling voids in a drusy quartz (qtz). Covellite is replaced by chalcocite (cc) associated with calcite (cal); e) *association III* composed veins of microcrystalline calcite (cal) and djurleite–chalcocite (dj–cc) euhedral crystals crosscutting brecciated pyrite (py); f) and g) *association III* formed by chalcocite (cc) and galena (gn) rims associated with calcite (cal); and h) aggregates of cinnabar (ci) and proustite (pr) filling fractures in massive pyrite (py).

(e.g. Tharsis; Tornos et al., 2008 and Aznalcollar; Almodóvar et al., 1998);

(iv) *Deformation.* The Las Cruces orebody was intensely deformed by folding and thrusting during the multi-stage Variscan deformation (Figs. 2, 3, 4a, b, c and d). In the IPB deposits, this deformation resulted in the fragmentation of the orebodies (e.g. Tharsis; Tornos et al., 2008) and/or their size increase due to tectonic stacking (e.g. Aznalcollar, Almodóvar et al., 1998);

Please cite this article as: Yesares, L., et al., The Las Cruces deposit, Iberian Pyrite Belt, Spain, Ore Geol. Rev. (2014), http://dx.doi.org/10.1016/j.oregeorev.2014.10.019

Table 3
Mineralogical patterns of Las Cruces gossan.

Mineral association	Mineralogy		Textures		Examples
	Relict	New-formed	Relict	New-formed	
Association I	qtz, (rt, ba)	gt I, hem I	*qtz:* brecciated; isolated fragments.	*gt I, hem I:* massive; colloform.	
Association II	qtz, gt I, hem I	gt II, hem I, sd I	*qtz:* brecciated; isolated fragments. *gt I, hem I:* isolated fragments; massive; colloform; nodules.	*sd I:* botroidal; microcrystalline; euhedral aggregates; filling fractures and voids. *gt II-hem II:* botroidal; filling fractures and voids. *sd I and gt II-hem II:* botroidal; banded; alternating microlayers.	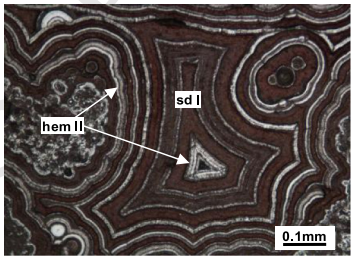
Association III	qtz, gt II, hem II, sd I (gt I, hem I)	sd II, cal, gn, py, (mrc, grei, po, Ag-sulfides, ci, amalgams)	*qtz:* brecciated; isolated fragments. *gt I, hem I:* isolated fragments; massive; colloform. *gt II, hem II, sd I:* botroidal; euhedral aggregates; alternating microlayers; filling fractures and voids.	*sd II:* microcrystalline; botroidal; euhedral aggregates. *py, mrc, grei, po:* euhedral–anhedral aggregates; colloforms; veinlets. *gn:* skeletal aggregates; veinlets; filling voids. *sd II and sulfides:* intergrowth; overgrowth; filling fractures and voids.	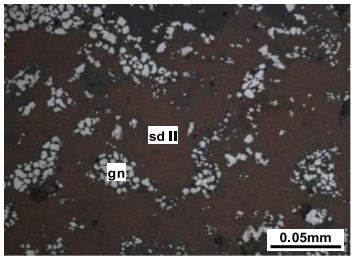

Mineral abbreviations: qtz—quartz; rt—ruttile; ba—barite; gt—goethite; hem—hematite; sd—siderite; py—pyrite; gn—galena; cal—calcite; mrc—marcasite; grei—greigite; po—pyrrhotite; ci—cinnabar.

(v) *Hydrothermal alteration.* Host rocks from the Las Cruces deposit, as occurs in most of the IPB massive sulfides, exhibit chloritic and/or quartz-sericitic hydrothermal alteration linked mostly in the stockwork zones (Sáez et al., 1999; Tornos, 2006).

(vi) *Mineralogy.* Ore minerals of the Las Cruces primary deposit include pyrite, and minor sphalerite, chalcopyrite, galena and tetrahedrite–tennantite. Bi–Cu-sulfosalts and arsenopyrite are also common (Figs. 6, 7a, b, c, d, e, f and Table 1). Similar ore mineral associations have been reported in most of the IPB deposit (Marcoux et al., 1996);

(vii) *Textures.* The main textures of the Las Cruces primary ore include: massive, disseminations, veinlets, filling voids, banded, framboidal, colloform, euhedral aggregates, recrystallization, overgrowth, intergrowth, segregations, brecciated, cataclastic and late-fracture filling (Fig. 7a, b, c, d, e, f and Table 1). Identical textural pattern has been also reported in neighboring deposits (e.g. Aznalcóllar; Almodóvar et al., 1998 and Massa Valverde; Ruiz et al., 2002);

(viii) *Zonations.* Despite the intense tectonic deformation affecting the Las Cruces orebody, an approximate zonation can be defined within the primary ore. This is characterized by a Cu-rich stockwork beneath the orebody flanked by zones with high Zn + Pb concentrations. In addition, pyrite zones are dispersed throughout the orebody. In the IPB deposit, this classical VMS zonation has been variously postulated (Franklin et al., 1981; Large, 1977; Routhier et al., 1978), although zonations are masked by intense deformation (Sáez et al., 1996; 1999; Almodóvar et al., 1998; Leistel et al., 1998; Relvas et al., 2001; Tornos, 2006);

(ix) *Geochemical features.* The IPB massive sulfides, including that of Las Cruces, show average low grades of base and precious metals (Sáez et al., 1999). The distribution of these elements throughout the Las Cruces primary sulfides is uneven. Pb, Zn and Ag concentrate mainly in polymetallic ores, whereas Cu values increase in the Cu-rich stockwork ore, in association with Bi. Higher Au concentrations have been found in both polymetallic and Cu-rich stockwork ores (Figs. 10, 11 and 12).

Concerning precious metals, Leistel et al. (1998) proposed two Au associations for the IPB deposits. The Tharsis–Sotiel–Migollas type, where Au occurs as electrum and concentrates in the stockwork zones associated with Co and Bi, and the Riotinto–Aznalcollar–La Zarza type, where Au is mainly concentrated in polymetallic ores associated with Zn, Ag, As, Tl and Hg, and appears as Ag–Hg-rich electrum and/or as auriferous arsenopyrite. The Las Cruces primary ores shows these two Au associations. Au show positive correlation with Ag and As as occur the Riotinto–Aznalcollar–La Zarza association type, and Au also shows positive correlation with Cu and Bi as in the Tharsis–Sotiel–Migollas association type (Figs. 10j, k and l).

7.2. Comparison with other supergene weathering profiles

The characteristic features of the Las Cruces deposit are typically represented by the secondary mineralization, including Cu-rich secondary sulfides and gossan. There are many differences and few similarities between the Las Cruces supergene profile and other weathered massive sulfides elsewhere (Jambor et al., 2000; Scott et al., 2001), including

Please cite this article as: Yesares, L., et al., The Las Cruces deposit, Iberian Pyrite Belt, Spain, Ore Geol. Rev. (2014), http://dx.doi.org/10.1016/j.oregeorev.2014.10.019

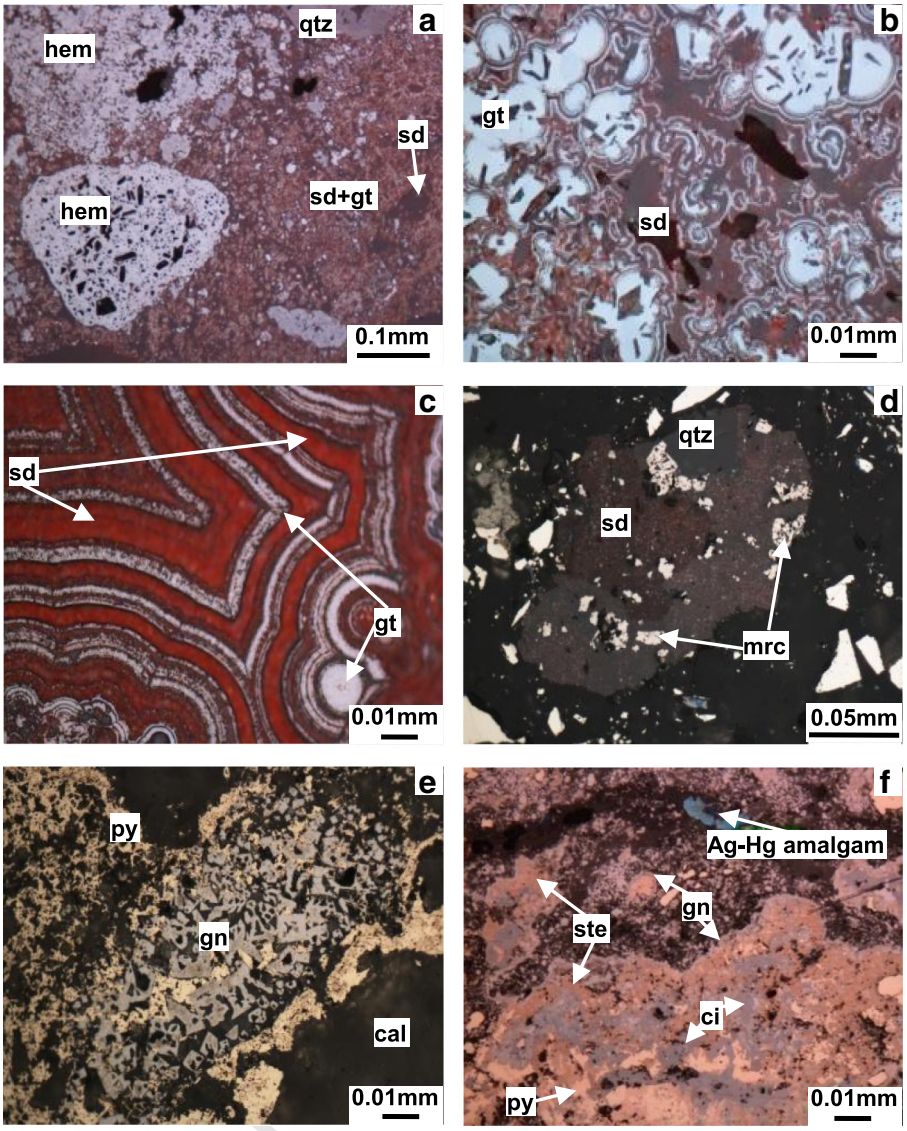

Fig. 9. Reflected light microscopy images of the Las Cruces gossan. a) *association I* composed of relicts of massive hematite (hem) cemented by microcrystalline siderite (sd) partially replaced by goethite (gt); b) *association II* formed by microcrystalline siderite (sd) replaced by botryoidal goethite (gt); c) *association II* comprised of microbands of alternating siderite (sd) and goethite (gt); d) and e) *association III* comprised of siderite (sd) and/or calcite (cc) and sulfides as pyrite (py), marcasite (mrc) and skeletal galena (gn); and f) massive stembergite (ste) and cinnabar (ci) cementing pyrite (py) relicts, fine veins of galena (gn) and Ag–Hg amalgams are observed as fillings voids.

those from the IPB (Capitán, 2006; Velasco et al., 2013). The most important differences and analogies between the Las Cruces weathering profile and other equivalent in the IPB and elsewhere are:

(i) *Tonnage and grades.* Compared with other IPB profiles, the Las Cruces gossan has a relatively minor size and higher grades (2 Mt @ 5.1 g/t Au and 155 g/t Ag). For example, the original resources of the Cerro Colorado gossan (Riotinto) exceeded 100 Mt @ 1 g/t Au and 56 g/t Ag, and those from the Filón Sur gossan (Tharsis) were of 15.5 Mt @ 1.7 g/t Au and 29 g/t Ag (Velasco et al., 2013). However, the Las Cruces cementation zone exhibits tonnage and grades relatively high (17.6 Mt @ 6.2% Cu). García Palomero (1992) estimated average grades of 3–5% Cu for cementation zones in the IPB deposits. No data of supergene tonnage from the IPB exist with which to compare that of Las Cruces, but published data on thickness evidence that the IPB supergene profiles range from the 3–4 m of Lagoa Salgada (Oliveira et al., 2011) to the 25 m of Cerro Colorado, Riotinto (García Palomero, 1992), whereas thickness of the Las Cruces cementation zone exceeds 50 m (Fig. 2);

(ii) *Contacts.* As other weathering profiles including those from the IPB, the top of the Las Cruces gossan is partially eroded, while the gossan footwall is in sharp contact with the cementation zone (Fig. 4a, b, c and d). In fracture-dominated zones, this contact is however more gradual. The cementation zone is in transitional contact with the underlying primary sulfides (Velasco et al., 2013; Yesares et al., 2010);

(iii) *Mineralogy.* The mineralogical composition of the Las Cruces supergene profile is the main distinguishing feature. Major minerals reported in gossans from the IPB and elsewhere include goethite, hematite, jarosite-group minerals and quartz (Capitán, 2006; Scott et al., 2001; Taylor and Thornber, 1992; Velasco et al., 2013). In contrast, the Las Cruces gossan is mostly formed by carbonates, Fe-sulfides and galena (Figs. 6, 9 and Table 3). Oxidized minerals such as Fe-oxyhydroxides and sulfates are lesser common and precious metals mainly occur as Au–Ag–Hg and Ag–Hg amalgams (Yesares et al., 2014). Similar mineralogical features have been reported in the Lagoa Salgada gossan, which also occurs buried beneath a thick post-alpine sedimentary cover (Oliveira et al., 2011). And analogous mineralogical

Please cite this article as: Yesares, L., et al., The Las Cruces deposit, Iberian Pyrite Belt, Spain, Ore Geol. Rev. (2014), http://dx.doi.org/10.1016/j.oregeorev.2014.10.019

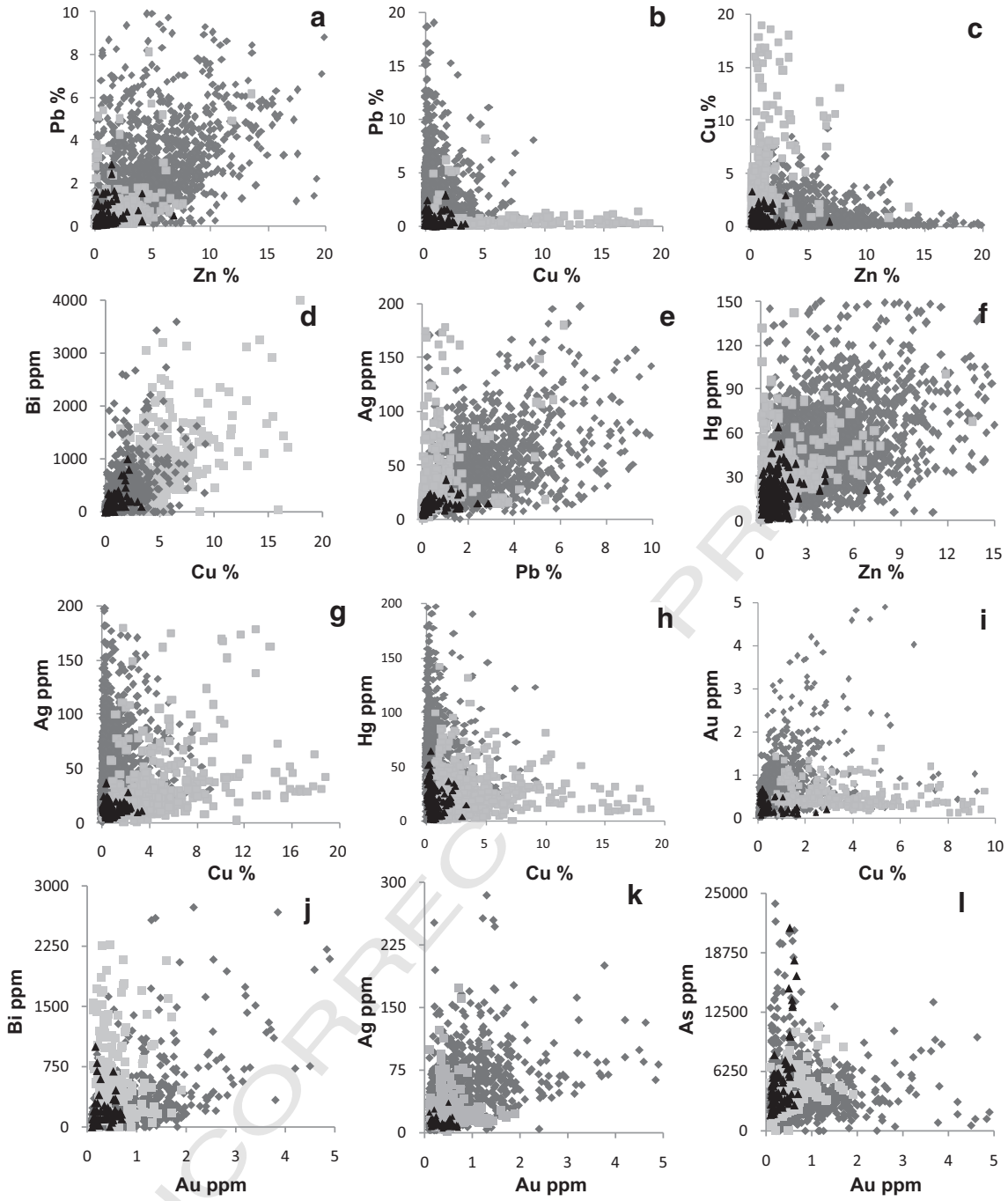

Fig. 10. Selected diagrams showing the main geochemical features of primary ore types at the Las Cruces deposit. Primary ores: ♦ polymetallic ore; ▪ Cu-rich ore; ▲ pyritic ore.

composition and geologic framework have been also reported for some gossans of VHMS deposits buried under Mesozoic–Cenozoic sediments at South Urals (Belogub et al., 2003, 2008). Concerning the cementation zone, Las Cruces shows similar mineralogical features (Fig. 8 and Table 2) to other VMS secondary sulfide-rich ores (e.g. Bathurst, Canadá; Boyle, 2003, Flambeau deposit, Wisconsin; May and Dinkowiz, 1996), and Lagoa Salgada in the IPB (Oliveira et al., 2011);

(iv) *Mineral association.* Mineral associations identified in the Las Cruces supergene profile are unusual. Early mineral associations from the gossan (Figs. 6, 9a and Table 3) and the cementation zone (Figs. 6, 8a, b, c and Table 2) developed by weathering under subaerial conditions, thus resembling those from other supergene profiles (Emmos, 1917; Sillitoe, 2005; Thornber, 1985). However, later mineral associations identified both in the cementation zone (Figs. 6, 8d, e, f, g and Table 2) and the gossan of Las Cruces (Figs. 6, 9b, c, d, e and Table 3), differ from those of the classical models (e.g. Scott et al., 2001; Sillitoe, 2005; Velasco et al., 2013). The main differences are related to the post-Variscan evolution under the Guadalquivir basin sedimentary cover;

(v) *Zonations.* According to Scott et al. (2001), weathering profiles from massive sulfide deposits typically show a vertical zonation characterized by several horizons. From bottom to top, they are: supergene sulfides, sulfate zone, carbonate zone, phosphate zone, ferruginous oxidized zone and gossan. By contrast, the weathering profile from the Las Cruces deposit only has three horizons: the Cu-rich supergene sulfides (Figs. 3, 5a, b, c and d),

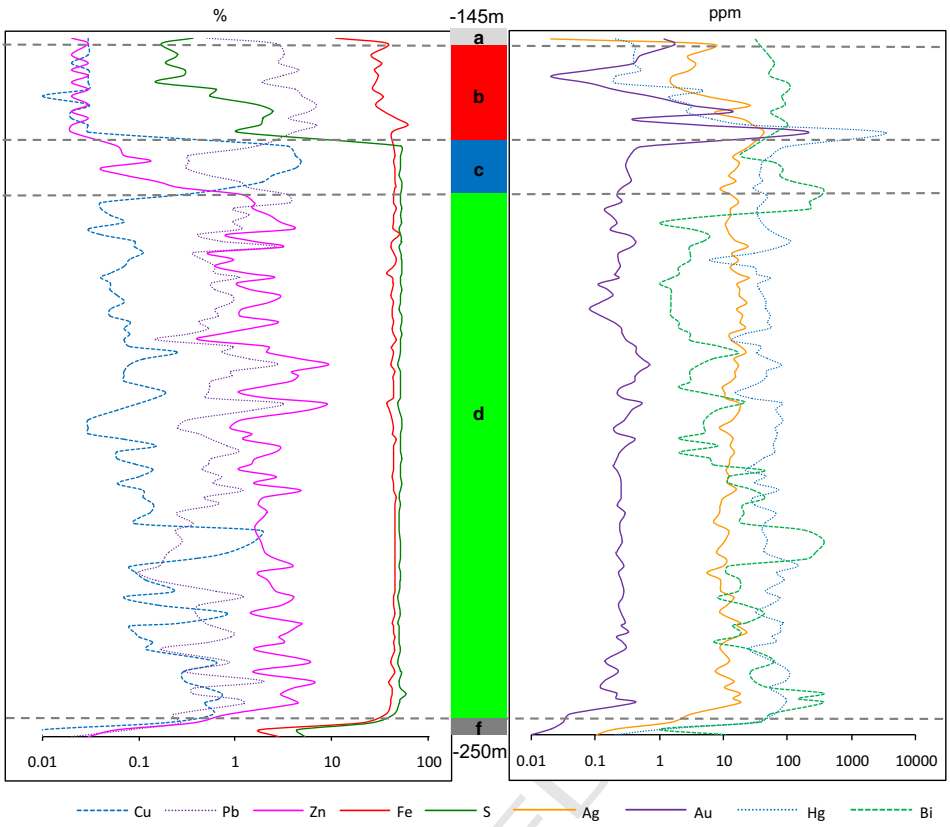

Fig. 11. Vertical distribution of metals at the Las Cruces deposit based on assays of drill hole no. CR277 (UTM coordinates: 757756, 4154790). a) sedimentary cover; b) gossan; c) cementation zone; d) polymetallic primary massive sulfide; and f) black shale host rocks.

which include an upper zone, 5-m-thick, of crumbled (sand-like) pyrite (Figs. 3, 4a, d and 5d), a thin sheared black shale level (Figs. 4a and 5e), interpreted as a redox front (Yesares et al., 2014), and the gossan (Figs. 3, 4a, b, c and d). Unlike other gossans from the IPB, which are normally zoned (Velasco et al., 2013), the Las Cruces gossan lacks internal structure and vertical zonation;

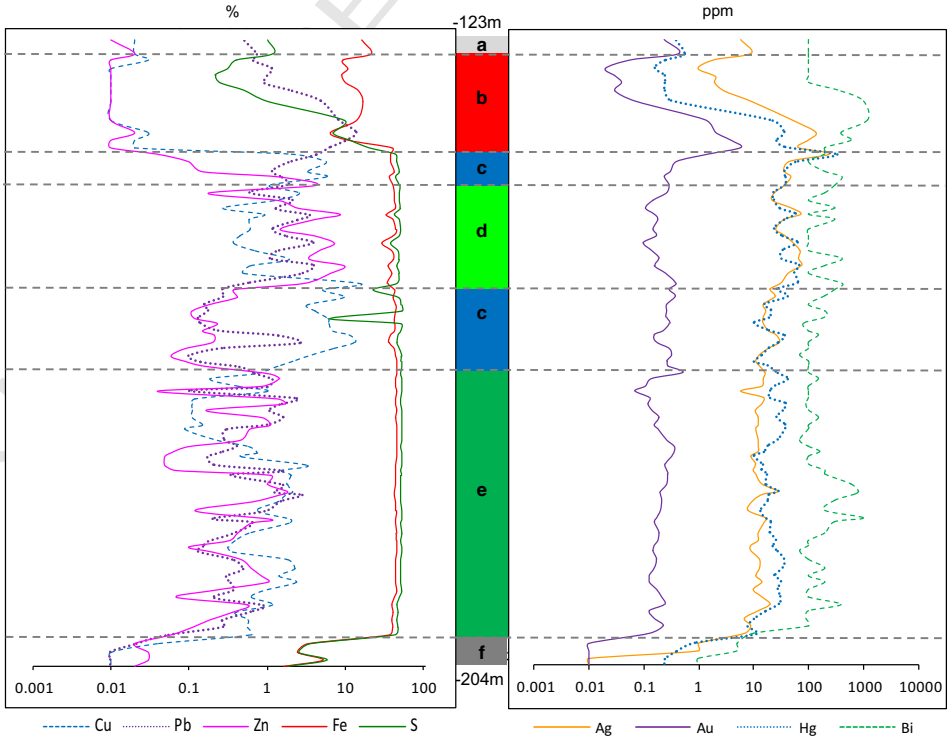

Fig. 12. Vertical distribution of metals at the Las Cruces deposit based on assays of drill hole no. CR258 (UTM coordinates: 757850.8, 4154850). a) sedimentary cover; b) gossan; (c) cementation zone; d) polymetallic primary mineralization; (e) pyritic primary mineralization; and f) black shale host rocks.

Please cite this article as: Yesares, L., et al., The Las Cruces deposit, Iberian Pyrite Belt, Spain, Ore Geol. Rev. (2014), http://dx.doi.org/10.1016/j.oregeorev.2014.10.019

Table 4
Summary geochemistry of the Las Cruces deposit.

Element (ppm)		No. of samples	Cu (%)			Pb (%)			Zn (%)			Au (ppm)			Ag (ppm)			Hg (ppm)		
			Min	Max	Mean	Min	Max	Mean	Min	Max	Mean	Min	Max	Mean	Min	Max	Mean	Min	Max	Mean
Primary ore	Pyritic	165	0.07	3.32	0.59	0.03	2.88	0.33	0.04	6.77	0.88	0.01	0.7	0.3	3.8	36.22	12.22	1.3	63.7	17.92
	Polymetallic	2056	0.01	9.2	0.81	0.05	27.2	2.12	0.02	27.36	4.27	0.1	8.37	0.72	0.4	713	42.35	0.3	814	52
	Cu-rich	540	0.1	18.9	3.99	0.1	8.11	0.57	0.1	13.6	1.4	0.1	1.9	0.53	0.1	293	28.4	0.1	141.1	26
Supergene Cu-enrichment		4854	0.1	39.5	6.55	0.1	39.98	0.76	0.1	36.91	0.44	0.1	285	0.62	0.1	1472	26.7	0.01	11,085	25
Gossan		2217	0.1	8.28	0.26	0.1	44.5	2.75	0.1	5.9	0.19	0.1	352.8	5.88	0.1	18,950	165.52	0.1	10,500	155

(vi) *Geochemistry.* Geochemical pattern of the Las Cruces gossan resembles those from other VHMS supergene profiles (Scott et al., 2001), including the IPB (Velasco et al., 2013). In the Las Cruces gossan S, Zn, and Cu (Figs. 11, 12 and Table 4) behaved as highly mobile elements that were leached out from the gossan during weathering. Conversely, Pb, Bi, Au, Ag and Hg are progressively enriched downward and concentrated at the bottom of the gossan (Figs. 11 and 12). A similar distribution has been reported in other IPB gossans (Capitán, 2006; Velasco et al., 2013), although the processes controlling such distribution seem to be less efficient in concentrating ore metals than in Las Cruces. There, the whole gossan has Pb, Au and Ag average values of 2.8 wt.% Pb, 2.5 ppm Au and 61.5 ppm Ag (Table 4), whereas in

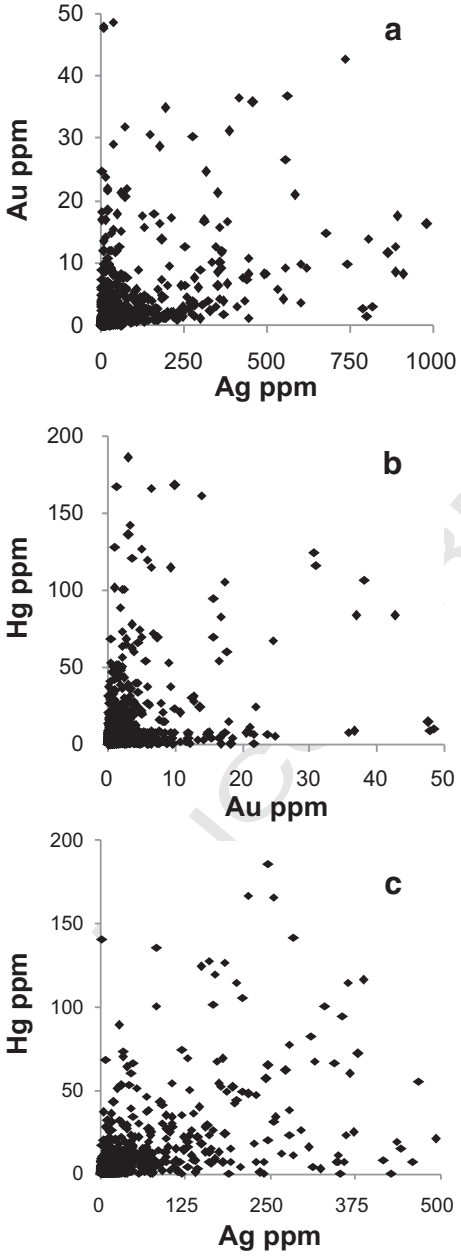

Fig. 13. Binary diagrams showing the main geochemical features of Las Cruces gossan.

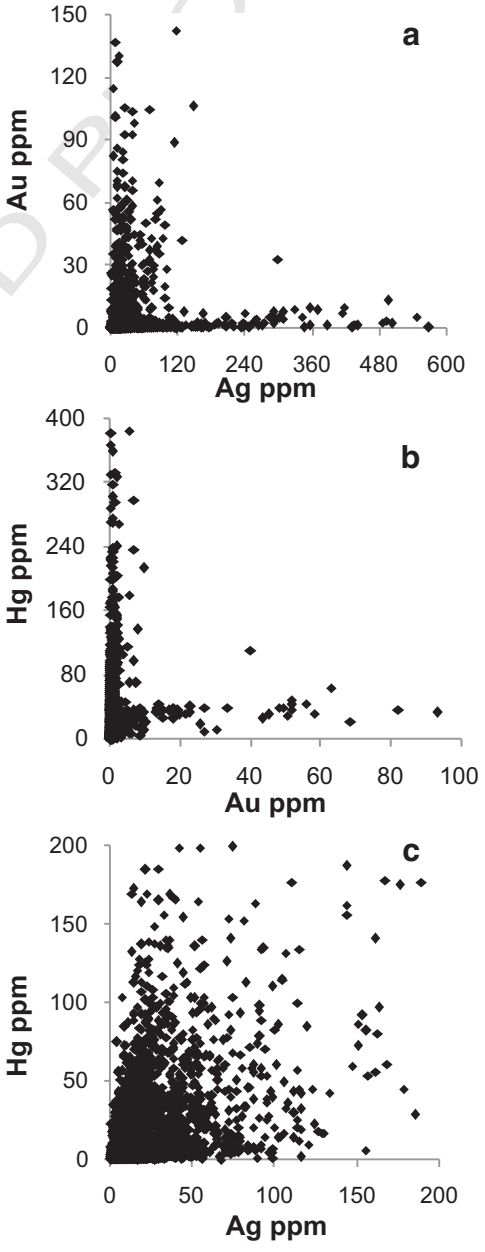

Fig. 14. Binary diagrams showing the main geochemical features of Las Cruces secondary copper mineralization.

the IPB those values are, respectively, 0.5 wt.% Pb, 1.5 ppm Au and 24 ppm Ag (Velasco et al., 2013). In any case, the main geochemical difference between Las Cruces and other gossans in the IPB concerns mainly with the geochemical behavior of Fe. While common IPB gossans have Fe average values of 39 wt.% (Velasco et al., 2013), that from Las Cruces is Fe-depleted, with average values of 15 wt.%.

7.3. Proposed genetic model

According to the data above and field observations, the following genetic and evolutionary model for the Las Cruces deposit is proposed (Fig. 15).

Genetic stage 1 Origin of the primary mineralization

As in other ore deposits in the IPB, the Las Cruces massive sulfide ore was deposited at the onset of the Variscan cycle, close to the Devonian-Carboniferous boundary (Nesbit et al., 1999; González et al., 2000; Nieto et al., 2000; Barrie et al., 2002). The extensional regime established in the region (Moreno et al., 1996; Saéz et al., 1996) produced the fragmentation of the IPB basin, favoring the ascent of magmas and the initiation of volcanism (Moreno et al., 1996).

At this stage, the pyritic sulfide association was generated (Figs. 6, 7a, b). The earlier stage of massive sulfide deposition, characterized by framboidal and colloform

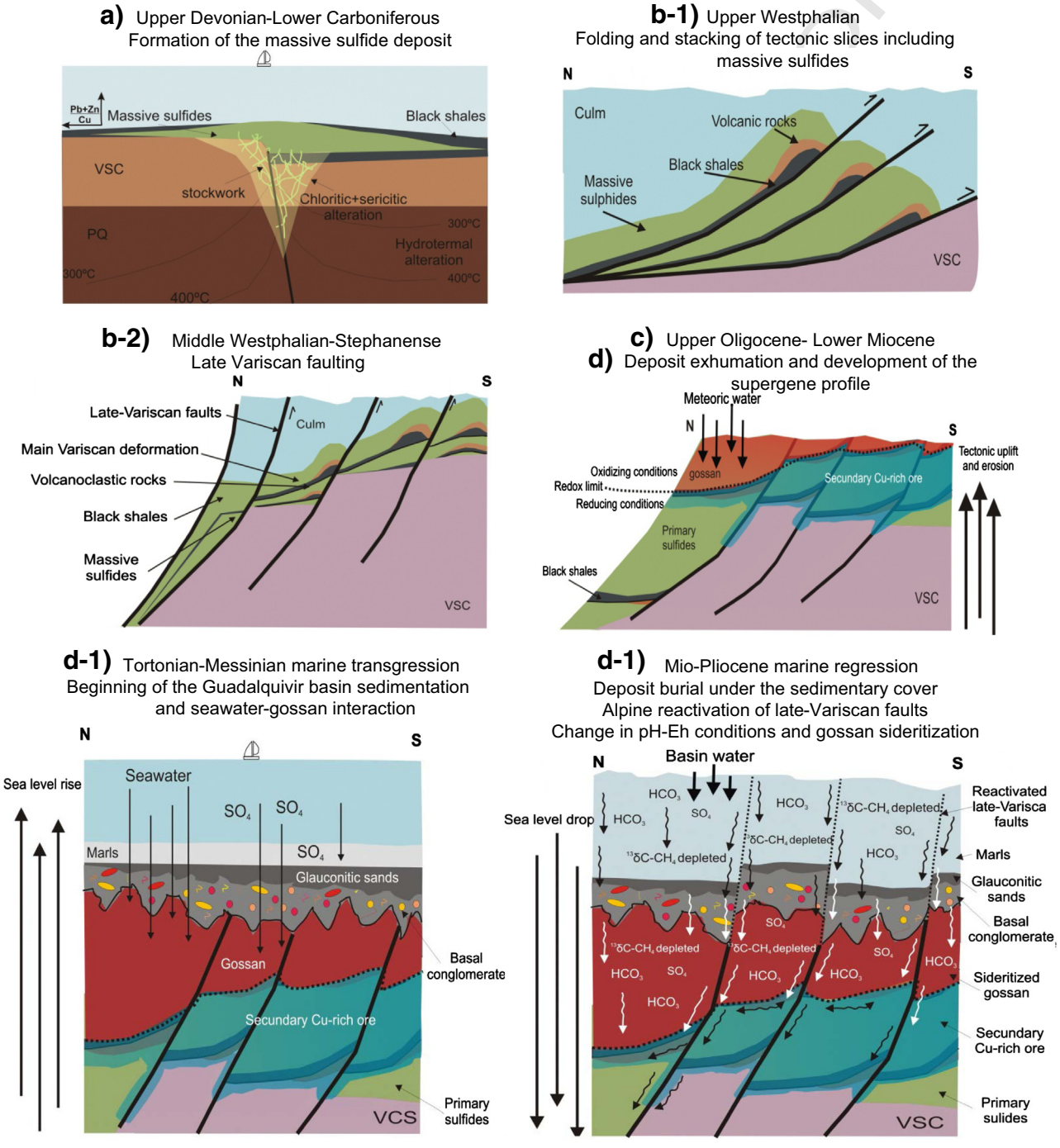

Fig. 15. Four-stage genetic model for the Las Cruces ore. a and b stages are based on common genetic models for IPB massive sulfide deposit.

Please cite this article as: Yesares, L., et al., The Las Cruces deposit, Iberian Pyrite Belt, Spain, Ore Geol. Rev. (2014), http://dx.doi.org/10.1016/j.oregeorev.2014.10.019

textures, occurred in a context of low-temperature diffuse fluid flow, immediately after deposition or early diagenesis of the host sediments, as occurred in other IPB deposits (e.g. Aznalcollar, Almodóvar et al., 1998; Tharsis, Sáez et al., 2011). Textural evidence suggests that framboids were formed by replacement of the original matrix, which probably comprised fine argillaceous material (Knigth, 2000), later hardened to form black shales.

Subsequently, the cyclical hydrothermal activity favored the generation of the polymetallic association. Textural evidence indicates that hydrothermal activity gradually increased, favoring the progressive deposition of sphalerite and galena, and favoring the development of the polymetallic massive sulfides facies as well as the pyrite recrystallization (Figs. 6, 7c, d).

Finally, the Cu-rich association containing Bi-minerals was generated (Figs. 6, 7e, f) in relation to late hydrothermal fluids associated with the stockwork zones. This ore type has been associated with high temperature conditions in other massive sulfides and stockwork type mineralizations all along the IPB (Marcoux et al., 1996).

Genetic stage 2 Variscan deformation

During Pennsylvanian times, the Variscan compressive tectonism produced the stacking of tectonic slices in the IPB (Simancas, 1983). The thin-skinned tectonic style produced the thrusting where the black shales and footwall chloritized rocks acted as detachment surfaces for the Variscan thrust system (Fig. 15b-1). Subsequently, during the last stage of Variscan deformation the Las Cruces ore deposit was affected by subvertical faulting (Figs. 2 and 15b-2).

Genetic stage 3 Genesis of the supergene profile

The exhumation of the IPB developed during Miocene (Velasco et al., 2013). In the Las Cruces area this resulted in the exhumation of the massive sulfides and the subsequent generation of gossan (Fig. 15c). There, the occurrence of gossan pebbles within the basal conglomerate level of the sedimentary cover (Fig. 5f) indicates that the weathering and oxidation of the massive sulfides predate the Tortonian (Moreno, 1993). These data are consistent with the age of 7.3 Ma (Jiménez-Moreno et al., 2013; Larrasoaña et al., 2008) assigned to the overlaying glauconitic sands (Fig. 4b, c and d).

Exposition of the Las Cruces deposit resulted in oxidation and leaching of part of the primary sulfides and the generation of the primary gossan (mineral association I) (Table 3 and Fig. 6). This consists mainly of iron oxyhydroxides (Figs. 6, 8a), Fe and Pb sulfates, and residual minerals such as quartz, cassiterite and rutile. The cementation zone was developed below the redox front. Mineral association I, identified into the cementation zone, represents the gradual supergene alteration of primary mineralization and the progressive replacement by secondary sulfides (Figs. 6, 7a, b and Table 2). By contrast, mineral association II corresponds to the direct precipitation of Cu-rich solutions leached down from an emergent gossan dominated by oxidation of primary sulfides (Figs. 6, 7c and Table 2).

Mineral associations of this stage described above are consistent with genetic models for supergene profiles based on the oxidation in subaerial conditions of precursor highly pyritic sulfides (Scott et al., 2001; Sillitoe, 2005). Production of sulfuric acid during pyrite oxidation causes intense leaching of the oxidized ore and promotes mobilization of metals into groundwater (Thornber, 1985). Under these conditions, immobile elements were concentrated in gossan, whereas mobile elements were transported and precipitated in secondary trap sites by means of cation-exchange reactions (Andrew, 1984; Sillitoe, 2005). The cementation zone was developed below the water table due to the precipitation of Cu-rich solutions and the generation of a wide variety of secondary Cu-rich mineral phases (Emmos, 1917; Sillitoe, 2005). The Cu-rich solutions leached from the oxidation zone, after breakdown of precursors Cu-sulfides.

During the oxidative dissolution of Fe-sulfides, Fe^{2+} is released in solution. Further oxidation in a reaction catalyzed by bacteria produces Fe^{3+} (McIntosh et al., 1997; Singer and Stumm, 1970), which remains in solution until pH reaches 3.5. Under these conditions iron is no longer stable in solution and precipitates as iron oxyhydroxi-sulfates (Bigham and Nordstrom, 2000; Thornber, 1985). Thus, part of the Fe is released in the acid rock drainage, and the other part is concentrated in situ in the gossan as Fe-bearing phases that remain stable in a wide range of pH conditions. Goethite dominates at pH values of 3–6, but is easily transformed to hematite by dehydration (Thornber and Wildman, 1984). The low Pb mobility under acid drainage processes (pH < 6) (Mann and Deutscher, 1980), favored the Pb enrichment of the Las Cruces gossan, with values up to 44.5 wt.%. Stable lead minerals during gossan formation include sulfo-arsenates of the jarosite group, phosphates, oxides and carbonates. This Pb enrichment has been reported in other weathering profiles and under laboratory conditions (Pirajno et al., 2010; Thornber, 1985). Under extremely acidic and oxidizing conditions, the Au liberated during the oxidative dissolution of sulfides, is oxidized to Au^{3+}, being able to be transported at short distances in association with ligands such as CN^{2-}, OH^{-}, NH_3, Cl^{-}, I^{-}, Br^{-}, and HS^{-} (Groen et al., 1990). The principal Au-fixing mechanism consists of the precipitation of native Au in association with Fe-oxyhydroxides (Mann, 1984; Stroffregen, 1986). Ag is more soluble under acidic oxidizing conditions (Krupp and Weiser, 1992), but is readily precipitated with a variety of secondary minerals such as halides, sulfates and sulfohalides (Dutrizac and Jambor, 1987; Saunders, 1993; Viñals et al., 1995). During the weathering of massive sulfides, Hg^{+} is oxidized to Hg^{2+}, and thus can be slightly mobilized as $HgCl_2^0$ through the profile. Such compound is stable in solution under acidic and oxidizing conditions (Davis et al., 1997). Cu and Zn are often totally leached away from the gossan due to their high mobility in acid waters, and in solutions containing sulfate, carbonate, and hydroxide and chloride anions (Mann and Deutscher, 1980). Cu ions leached from gossan remain in solution at pH < 5.5 (Bloom, 1966) and descent to the water table where the slightly reducing conditions favor re-precipitation of electropositive metals (Sato, 1992).

Genetic stage 4 Profile evolution below the sedimentary cover

During the Alpine orogeny, the tectonic subsidence produced an ongoing sea level rise in the Miocene. The maximum transgressive and subsident stage was

Please cite this article as: Yesares, L., et al., The Las Cruces deposit, Iberian Pyrite Belt, Spain, Ore Geol. Rev. (2014), http://dx.doi.org/10.1016/j.oregeorev.2014.10.019

reached at the Tortonian–Messinian boundary, given rise to the sedimentation in the passive margin of the Guadalquivir Basin (Abad, 2007). In consequence, the Las Cruces ore deposit, including the supergene profile, was gradually buried by the sediments associated with such transgression (Fig. 15d-1).

The beginning of the sedimentation stars with the erosion of the hanging wall of the Las Cruces gossan, the deposition of the basal conglomerate and the overlying calcareous sediments at the early Tortonian. Eroded gossan pebbles were then incorporated in the so called basal conglomerate level (Moreno et al., 2002) (Fig. 5f). Somewhat later, the Tortonian–Messinian maximum transgressive resulted in the sedimentation of glauconitic sands and marls (Fig. 15d-1). The Miocene seawater–gossan interaction and the halmyrolysis-related process took place during this stage. They are consistent with the presence of newly-formed kaolinite and smectite in the gossanized host rocks (Yesares et al., 2014) and the highly enriched $\delta^{34}S$ values of the supergene sulfides (as discussed below).

During Mio-Pliocene boundary, the end of the tectonic subsidence took place, resulting in the marine regression. At this time, the supergene profile remains entirely beneath the redox front, and hence under reducing conditions (Fig. 15d-2). Mineral associations II and III of gossan (Figs. 6, 9b, c, d, e and Table 3) and association III of the secondary Cu-rich zone (Figs. 6, 7d, e, f, g and Table 2) are interpreted in relation to the ore burial under the sedimentary cover. Mineralogical and textural features, together with geochemical data, suggest that the topographic and climatic condition at Las Cruces area favored the progressive changes of the hydrogeological flow pattern. Eh-pH conditions of the Las Cruces water environment were progressively more reducing due to the rise of the redox front, and more alkaline as a result of the circulation of meteoric fluids equilibrated with the carbonates of the sedimentary pile. The late Variscan faults, reactivated during the Alpine orogeny, generated highly permeable zones through which the pervasive water circulated to the sediments–gossan interface (Fig. 15d-2).

In this stage, the carbonatization of the oxyhydroxides at the gossan and the reduction of Fe^{3+} to Fe^{2+} produced respectively the precipitation of siderite and Fe-sulfides in the gossan (Figs. 6, 9,b, c and d), and the release of Fe^{2+}, much more mobile than Fe^{3+} (Stumm and Morgan, 1996). The change from oxidizing to reducing conditions, and the reductive dissolution of those sulfates hosted in the overlying sediments and from the gossan itself, also favored the generation of galena in the gossan due to the precipitation of Pb-oxysalts during ore burial (Figs. 6 and 9e).

Circulation of fluids saturated in carbonates through the cementation zone increased progressively the pH, thus altering the first generation of secondary Cu-sulfides (Garrels and Christ, 1965; Sato, 1992), and transforming these in a second generation of Cu-sulfides, associated to carbonates and other newly-formed sulfides such as galena and pyrite (Figs. 6, 8d, e, f and g).

Changes in Eh-pH conditions of the descending fluids produced several dissolution–precipitation cycles of Au, Ag and Hg as amalgams, cinnabar and Ag-sulfides, and favored the precious metals enrichment near the gossan base (Yesares et al., 2014).

Even though the burial of the supergene profile under the sedimentary pile led to suitable reducing and alkaline conditions for carbonates and sulfides generation, other factors must be considered to explain the Las Cruces patterns. For instance, the $\delta^{13}C$ isotope composition reported for carbonates in the Las Cruces gossan ranges between −13.4‰ and −47.95‰, averaging −25.2‰ (Capitán, 2006). An extremely complex "bio-reactor" model has recently been proposed to explain theses $\delta^{13}C$ strongly negative values. This model involves methanogenesis processes linked to in situ biological activity which generate CO_2/HCO_3, CH_4 and H_2S/HS^- resulting in the generation of newly-formed carbonates and sulfides at the gossan (Blake, 2008; Tornos et al., 2014).

However, such in situ biological activity is not the only possible source of methane in the Las Cruces area. It is widely known that the sedimentary pile of the Guadalquivir Basin contains large accumulations of organic matter and biogenic hydrocarbons (Lunar et al., 2002; Melendez-Hevia and Alvarez del Buergo, 1996) which have even resulted in hydrocarbon deposits of economic interest. Very light $\delta^{13}C$ values have been reported from hydrocarbons hosted in sediments, with values even lower than −91‰ VPDB (Hoefs, 1987; Schoell, 1979). In that sense, Nuzzo et al. (2009) reported a $\delta^{13}C$–CH_4 composition ranging between −73.3 and −33.8‰ VPDB in pore water sediments of the Gulf of Cádiz. Therefore, the thick sedimentary cover in the Las Cruces area is a plausible reservoir of organic matter, methane and other gases with depleted $\delta^{13}C$ values. In addition, the sedimentary cover is hydraulically connected with the gossan deposit through a pervasive fracture set, which could be the pathway linking the basinal waters and the gossan profile. These water–rock interaction mechanisms could result in the precipitation of depleted $\delta^{13}C$ carbonates derived from the Miocene marine waters and the associated hydrocarbon-rich sediments (Fig. 15d-2).

Moreover, the published $\delta^{34}S$ composition of the Las Cruces supergene profile is extremely heavy. Galena and Fe-sulfides of the gossan and the late generation of supergene Cu-sulfides in the cementation zone show $\delta^{34}S$ mean values of 19.4 ± 3.5‰, 17.8 ± 1.2‰ and 12.8 ± 5.2‰ respectively, whereas the $\delta^{34}S$ composition of the primary sulfides exhibits average values of 5.9 ± 3.6‰ (Knigth, 2000; Tornos et al., 2014). This $\delta^{34}S$ extreme enrichment in the secondary ores is unlikely to occur by bacterial activity, as proposed by Tornos et al. (2014). The biogenic sulfate-reduction processes generally result in a depletion of the original $\delta^{34}S$ composition, reaching even negative values (Bawden et al., 2003; Fallick et al., 2001). Therefore, this $\delta^{34}S$ enrichment, both in the gossan and in the secondary Cu-rich ores, requires a different heavy S source. The most suitable source for such heavy S seems to be the sulfate-rich seawaters during the Miocene marine transgression and the pore fluids within the hanging wall sedimentary pile (Fauré, 1986; Hoefs, 1987) (Fig. 15d-2). In this way, a progressive addition of S derived from the reduction of Miocene seawater sulfates could lead to the increase of $\delta^{34}S$ values.

Please cite this article as: Yesares, L., et al., The Las Cruces deposit, Iberian Pyrite Belt, Spain, Ore Geol. Rev. (2014), http://dx.doi.org/10.1016/j.oregeorev.2014.10.019

8. Conclusions

The data exposed in this paper suggest that the Las Cruces primary sulfide ores closely resemble other VMS deposits, but its weathering profile however includes features uncommon for these deposits.

Those features shared with other VMS deposits include: mineralogy, tectonic style, nature of host rock, geochemical zonation and mineralization types. The main differences center on the supergene weathering profile, dealing essentially with geometrical characteristics such as internal structure or thickness of the supergene Cu enrichment zone, and with mineralogical features related to the generalized occurrence of reduced phases in the gossan. In mining terms, such peculiarities have consequences in relation to unusual tonnage and grades.

The most significant difference within the supergene profile deals with the mineralogy. The first mineralogical associations occurring at the cementation zone and gossan are related to the weathering of primary sulfides at subaerial conditions. These associations have been usually described in other supergene profiles. Nevertheless, the subsequent mineralogical associations are rarely matched in other comparable deposits.

Based on the data and interpretations discussed above, we propose a genetic model for the genesis of the Las Cruces ore deposit that suggests strong similarities with other IPB deposits in the generation of the primary sulfides, and also explain the anomalies in the weathering profile related to the Miocene marine incursion and the later evolution of the deposit below the sedimentary cover. The Tortonian–Messinian transgressive–regressive events produced changes in the hydrological flow and the physico-chemical environmental conditions. All these changes affected the water–rock interaction processes resulting in two different ore-generation stages in the Las Cruces supergene profile: (1) subaerial oxidation and leaching of a portion of the primary sulfides. This resulted in the generation of iron oxyhydroxides in the vadose zone, which produced primary gossan, the gradual supergene alteration of primary mineralization, and the precipitation of Cu-rich solutions and generation secondary Cu-sulfides in the saturated zone. Those first genetic patterns are better preserved in the cementation zone; and (2) Miocene marine events and the associated sedimentation in produced the Las Cruces area the seawater–gossan interaction and the later buffering of basin solutions. These processes favored the gossan reduction and the replacement of early-oxidized minerals by siderite, Fe-sulfides and galena in the gossan, and the reactivation of the cementation zone resulting in a second generation of Cu-sulfides associated to carbonates, Ag-sulfides and cinnabar.

9. Uncited references

Q37

Essalhi et al., 2011
Lecolle, 1977
Strauss et al., 1981

Acknowledgment

This research is a contribution to projects P-S Anoxia (CGL2011-30011) and Metodica (CGL2010-21956-C02-02), which are supported by the Spanish Government (MINECO). The authors thank COBRE LAS CRUCES S.A. for the field assistance, the ongoing collaboration and for the permission to publish data acquired in the exploration stage. We are also grateful to Felipe González for their improving language suggestions. The comments and corrections of Eric Marcoux and an anonymous reviewer clearly enhanced the quality of the manuscript.

Q38

References

Abad, M., 2007. La transgresión Tortoniense en el margen pasivo de la Cuenca del Guadalquivir: Unpublished PhD Thesis. University of Huelva, Spain.
Almodóvar, G.R., Pascual, E., Sáez, R., Toscano, M., 1997. Eastern Iberian Pyrite Belt (Spain): Tharsis, Riotinto and Aznalcóllar. In: Barriga, F.J.A.S., Carvalho, D. (Eds.), Geology and VMS deposits of the Iberian Pyrite Belt. Guidebook prepared for the Society of Economic Geologists Field Conference (7–17 May 1997) (Guide book Series. 27).
Almodóvar, G.R., Sáez, R., Pons, J.M., Maestre, A., Toscano, M., Pascual, E., 1998. Geology and genesis of the Aznalcollar massive sulphide deposits, Iberian Pyrite Belt, Spain. Miner Deposita 33, 111–136.
Álvaro, A., Velasco, F., 2002. Etapas de alteración supergénica en la formación del gossan de San Miguel (FPI). Bol Soc Esp Mineral 25A, 3–4.
Amorós, J.L., Lunar, R., Tavira, P., 1981. Jarosite: a silver bearing of the gossan of Río Tinto (Huelva) and La Unión (Cartagena). Miner Deposita 16, 205–213.
Andrew, R.L., 1984. The geochemistry of selected base-metal gossans, Southern Africa. J Geochem Explor 22, 161–192.
Arribas, A., 1998. Los yacimientos de oro asociados con las monteras limoníticas de la FPI. Bol Geol Min 109 (5-6), 429–434.
Aye, F., 1974. Géologie et gîtes métalliferes de la moyenne vallée de l'Odiel (Huelva, Espagne): relations entre la gènese des amas pyriteux cupifères, stratiformes, et celle de leur enveloppe volcanosédimentaire dévono-dinantienne(PhD Thesis) University Pierre et Marie Curie, Paris (France).
Barrie, C.T., Amelin, Y., Pascual, E., 2002. U–Pb geochronology of VMS mineralization in the Iberian Pyrite Belt. Miner Deposita 37, 684–703.
Barriga, F.J.A.S., 1990. Metallogenesis in the Iberian Pyrite Belt. In: Dallmeyer, R.D., y Martínez-García, E. (Eds.), Pre-Mesozoic Geology of Iberia. Springer-Verlag, Berlin, Heidelberg, New York.
Bawden, T.M., Einaudi, M.T., Benjamin, C., Bostick, Meibom, A., Wooden, J., Norby, J.W., Orobona, M.J.T., Chamberlain, C.P., 2003. Extreme S-34 depletions in ZnS at the Mike gold deposit, Carlin trend, Nevada: evidence for bacteriogenic supergene sphalerite. Geology 31, 913–916.
Belogub, E., Novoselov, C., Spiro, B., Yakovleva, B., 2003. Mineralogical and sulphur isotopic features of the supergene profile of Zapadno-Ozernoye massive sulphide and gold bearing gossan deposit, South Urals. Miner Mag 67, 339–354.
Belogub, E.V., Novoselov, K.A., Yakovleva, V.A., Spiro, B., 2008. Supergene sulphides and related minerals in the supergene profiles of VHMS deposits from the South Urals. Ore Geol Rev 33, 239–254.
Bigham, J.M., Nordstrom, D.K., 2000. In: Alpers, C.N., Jambor, J.L., Nordstrom, D.K. (Eds.), Iron and aluminum hydroxysulfates from acid sulfate waters, in Sulfate Minerals: crystallography, geochemistry & environmental significance. Rev. Mineral. Geochem. 40, pp. 303–350.
Blain, C.F., Andrew, R.L., 1977. Sulphide weathering and the mineral evaluation of gossan in mineral exploration. Miner Sci Eng 9, 119–150.
Blake, C., 2008. The mineralogical characterisation and interpretation of a precious metal-bearing fossil gossan, Las Cruces, Spain: Unpublished PhD Thesis. Cardiff: University of Wales.
Bloom, H., 1966. Geochemical exploration as applied to copper-molybdenum deposits. In: Titley, S.R., Hicks, C.L. (Eds.), Geology of the Porphyry Copper Deposits, South Western North America. University of Arizona Press, Tucson, pp. 111–119.
Boyle, D.R., 2003. Preglacial weathering of massive sulfide deposits in the Bathurst Mining Camp: economic geology, geochemistry, and exploration applications. In: Goodfellow, W.D., McCutcheon, S.R., Peter, J.M. (Eds.), Massive Sulphide Deposits of the Bathurst Mining Camp, New Brunswick, and Northern Maine. Econ. Geol. Monogr. 11, pp. 689–721.
Capitán, M.A., 2006. Mineralogía y geoquímica de la alteración superficial de depósitos de sulfuros masivos en la Faja Pirítica Ibérica: Unpublished PhD Thesis. University of Huelva, Spain.
Capitán, M.A., Nieto, J.M., Sáez, R., Almodóvar, G.R., 2003. Caracterización textural y mineralógica del gossan de Filón Sur (Tharsis, Huelva). Bol Soc Esp Miner 26, 45–58.
Carvalho, D., Ferreira, A., 1993. Geologia de Neves-Corvo: estado actual do conhecimento. Symp. Polymetallic Sulphides of the Iberian Pyrite Belt, Évora, Portugal.
Carvalho, D., Barriga, F.A.S., Munhá, J., 1999. Bimodal siliciclastic systems, the case of the Iberian Pyrite Belt. In: Barrie, C.T., Hannington, M.D. (Eds.), Volcanic-associated Massive Sulfide Deposits: Processes and Examples in Modern and Ancient Settings. Rev. Economic Geology 8, pp. 375–408.
Davis, A., Bloom, N.S., Shane, S., Hee, Q., 1997. The environmental geochemistry and bioaccessibility of Hg in soils and sediments. Risk Anal 17, 557–569.
Doyle, M., Morrissey, C., Sharp, G., 2003. The Las Cruces Orebody, Seville province, Andalucia, Spain. In: Kelly, C.G., et al. (Eds.), The Geology and Genesis of Europe's Major Base Metal Deposits. Irish Association for Economic Geology, Dublin, pp. 381–390.
Dutrizac, J.E., Jambor, J.L., 1987. Behaviour of Ag during jarosite precipitation: T. I. Min Metall 80, 206–218.
Emmos, W.H., 1917. The enrichment of ore deposit. US Geol Surv Bull 625 (530 pp.).
Essalhi, M., Sizaret, S., Barbanson, L., Chen, Y., Lagroix, F., Demory, F., Nieto, J.M., Sáez, R., Capitán, M.A., 2011. A case study of the internal structures of gossans and weathering processes in the Iberian Pyrite Belt using magnetic fabrics and paleomagnetic dating. Miner Deposita 46, 981–999.
Fallick, A.E., Ashton, J.H., Boyce, A.J., Ellam, R.M., Russell, M.J., 2001. Bacteria were responsible for the magnitude of the world class hydrothermal base metal sulfide orebody at Navan, Ireland. Econ Geol 96, 885–890.
Fauré, G., 1986. Principles of Isotope Geology, 2 ed. John Wiley and Sons, New York (589 pp.).
Franklin, J.M., Sangster, D.F., Lydon, J.W., 1981. Volcanogenic massive sulphide deposits. Econ Geol 485-627 (75th Anniv.).
Franklin, J.M., Gibson, H.L., Galley, A.G., Jonasson, I.R., 2005. Volcanogenic massive sulfide deposits. In: Hedenquist, J.W., Thompson, J.F.H., Goldfarb, R.J., Richards, J.P. (Eds.), Economic Geology 100th Anniversary Volume. Society of Economic Geologists, Littleton, CO, pp. 523–560.
García de Miguel, J.M., 1990. Mineralogía, paragénesis y sucesión de los sulfuros masivos en la Faja Pirítica en el suroeste de la Península Ibérica. Bol Geol Min 101, 73–105.

Please cite this article as: Yesares, L., et al., The Las Cruces deposit, Iberian Pyrite Belt, Spain, Ore Geol. Rev. (2014), http://dx.doi.org/10.1016/j.oregeorev.2014.10.019

García Palomero, F., Bedia Fernández, J.L., García Magariño, M., Sides, E.J., 1986. Nuevas investigaciones y trabajos de evaluación de reservas de gossan en Minas de Riotinto. Bol Geol Min XCVII, 622–642.
Garrels, R.M., Christ, C.L., 1965. In: Harper, Row (Ed.), Solutions, Minerals and Equilibria.
González, F., Moreno, C., López, M.J., Dino, R., Antonioli, L., 2004. Palinoestratigrafía del Grupo Pizarroso-Cuarcítico del sector más oriental de la Faja Pirítica Ibérica, SO de España. Rev Esp Micropaleontol 26, 279–304.
González-Delgado, J.A., Civis, J., Dabrio, C.J., Goy, J.L., Ledesma, J., Pais, J., Sierro, F.J., Zazo, C., 2004. Cuenca del Guadalquivir. In: Vera, J.A. (Ed.), Geología de España. SGE-IGME, Madrid, pp. 543–550.
Groen, J.C., Craig, J.R., Rimstidt, J.D., 1990. Au-rich rim formation on electrum grains in placers. Can Mineral 28, 207–228.
Hannington, M.D., Scott, S.D., 1989. Sulfidation equilibria as guides to gold mineralization in volcanogenic massive sulfides; evidence from sulfide mineralogy and the composition of sphalerite. Econ Geol 84, 1978–1995.
Herzig, P.M., Hannington, M.D., 1995. Polymetallic massive sulfides at the modern sea floor. A review. Ore Geol Rev 10, 95–115.
Hoefs, J., 1987. Stable Isotope Geochemistry, 3rd ed. Springer-Verlag, Berlín.
Jambor, J.L., Nordstrom, D.K., Alpers, C.N., 2000. In: Alpers, C.N., Jambor, J.L., Nordstrom, D.K. (Eds.), Metal-sulfate salts from sulphide mineral oxidation, in sulfate minerals: crystallography, geochemistry & environmental significance. Rev. Mineral. Geochem. 40, pp. 303–350.
Jiménez-Moreno, G., Pérez-Asensio, J.N., Larrasoaña, J.C., Aguirre, J., Civis, J., Rivas-Carballo, M.R., Valle-Hernández, M.F., González-Delgado, J.A., 2013. Vegetation, sea-level and climate changes during the Messinian salinity crisis. Geol Soc Am Bull 125, 432–444.
Julivert, T.M., Fontboté, J.M., Ribeiro, A. and Conde, L., 1974. Mapa tectónico de la Península Ibérica y Baleares. Escala 1:1,000,000. Ins. Geol. Min. Esp.
Knigth, F., 2000. The mineralogy, geochemistry and genesis of the secondary sulphide mineralization of the Las Cruces Deposit, Spain: Unpublished PhD Thesis. Cardiff: University of Wales.
Kosakevitch, A., García Palomero, F., Leca, X., Leistel, J.M., Lenotre, N., Sobol, F., 1993. Contrôles climatique et géomorphologique de la concentration de l'ordans les chapeaux de fer de Rio Tinto (Province de Huelva, Espagne). C R Acad Sci Paris 316, 85–90.
Kosakevitch, A., Leca, X., Leistel, J.M., Lenotre, N., García Palomero, F., Sobol, F., 1994. Climatic and geomorphological controls on the gold concentration of the Rio Tinto gossans: BRGM. Doc. In: Leistel, et al. (Eds.), The Massive Sulphide Deposits of the South Iberian Pyrite Province: Geological Setting and Exploration Criteria. 234, pp. 163–236.
Krupp, R.E., Weiser, T., 1992. On the stability of Au–Ag alloys in the weathering environment. Miner Deposita 27, 268–275.
Large, R.R., 1977. Chemical evolution and zonation of massive sulfide deposits in volcanic terrains. Econ Geol 72, 549–572.
Larrasoaña, J.C., Roberts, A.P., Rohling, E.J., 2008. Magnetic susceptibility of eastern Mediterranean marine sediments as a proxy for Saharan dust supply? Mar Geol 254, 224–229.
Lecolle, M., 1977. La ceinture sud-ibérique: un exemple de province à amas sulfures volcano-sedimentaires. Thèse, Université et M. Curie, Paris (609 pp).
Lécolle, M., Roger, G., 1973. Metallotects lithostratigraphiques et paleogeographiques dans la province pyritocupifere sud-iberique. C R Acad Sci Paris 276, 141–144.
Leistel, J.M., Bonijoly, D., Braux, C., Freyssinet, P., Kosakevitc, A., Leca, X., Lescuyer, J.L., Marcoux, E., Milési, J.P., Piantone, P., Sobol, F., Tegyey, M., Thieblemont, D., Viallefond, L., 1994. The massive sulphide deposits of the South Iberian Pyrite Province: geological setting and exploration criteria. pp. 234–236, (BRGM. Doc).
Leistel, J.M., Marcoux, E., Thiéblemont, D., Quesada, C., Sánchez, A., Almodóvar, G.R., Pascual, E., Sáez, R., 1998. The volcanic-hosted massive sulfide deposits of the Iberian Pyrite Belt. Review and preface to the Thematic Issue. Miner Deposita 33, 2–30.
Lunar, R., Moreno, T., Lombardero, M., Regueiro, M., López-Vera, F., Martínez del Olmo, W., Mallo, J.M., Saenz, J.A., García-Palomero, F., Higueras, P., Ortega, L., Capote, R., 2002. In: Gibbons, W., Moreno, T. (Eds.), The Geology of Spain, The Geological Society.
Mann, A.W., 1984. Mobility of Au and Ag in lateritic weathering profiles: some observations from Western Australia. Econ Geol 79, 38–50.
Mann, A.W., Deutscher, R.L., 1980. Solution geochemistry of lead and zinc in water containing carbonate, sulphate and chloride ions. Chem Geol 29, 293–311.
Marcoux, E., Moelo, Y., Leistel, J.M., 1996. Compared ore mineralogy and geochemistry of the massive sulfide and stringer ore deposits of the Southern Spain. Miner Deposita 31, 1–26.
May, E.R., Dinkowiz, S.R., 1996. An overview of the Flambeau supergene enrichment massive sulphide deposit: geology and mineralogy, Rusk County, Wisconsin. In: La Berge, G.L. (Ed.), Volcanogenic Massive Sulphide Deposits of Northern Wisconsin. 42, pp. 67–93.
McIntosh, J.M., Silver, M., Groat, L.A., 1997. Bacteria and the breakdown of sulfide minerals. Mineralogical Association of Canada Short course 25, pp. 63–92.
Melendez-Hevia, E., Alvarez del Buergo, E., 1996. In: Friend, P.F., Dabrio, C.J. (Eds.), The Stratigraphic Record of Crustal Kinematics. Cambridge University Press, Tertiary Basins of Spain, pp. 20–23.
Mitjavila, J., Martí, J., Soriano, C., 1997. Magmatic evolution and tectonic setting of the Iberian Pyrite Belt Volcanism. J Petrol 38, 727–755.
Moreno, C., 1987. Las facies del Culm del anticlinorio de La Puebla de Guzmán (Huelva, España)(PhD Thesis) University of Granada, Spain.
Moreno, C., 1993. Postvolcanic Paleozoic of the Iberian Pyrite Belt: an example of basin morphologic control on sediment distribution in a turbidite basin. J Sed Petrol 63, 1118–1128.
Moreno, C., Saéz, R., 1990. Sedimentación marina somera en el devónico del Anticlinorio de Puebla de Guzmán, Faja Pirítica Ibérica. Geogaceta 8, 62–64.
Moreno, C., Sequeiros, L., 1989. The Basal Shaly Fm of Iberian Pyrite Belt (South Portuguese Zone): Early Carboniferous bituminous deposits. Palaeogeogr Palaeoclimatol Palaeoecol 73, 233–341.
Moreno, C., Sierra, S., Saéz, R., 1996. Evidence for catastrophism at the Famennian–Dinantian boundary in the Iberian Pyrite Belt. In: Storgen, P., Sommerville, I.D., Jones, J.L. (Eds.), Recent Advances in Lower Carboniferous Geology. Geological Society. Spec. Publ 107, pp. 153–162.
Moreno, C., Capitán, M.A., Doyle, M., Nieto, J.M., Ruiz, F., Sáez, R., 2002. Edad mínima del gossan de Las Cruces: implicaciones sobre el inicio de los ecosistemas extremos en la Faja Pirítica Ibérica. Geogaceta 33, 67–70.
Nesbit, R.W., Pascual, E., Fanning, C.M., Toscano, M., Sáez, R., Almodóvar, G.R., 1999. U–Pb dating of stockwork zircons from the Eastern Iberian Pyrite Belt. J Geol Soc London 156, 7–10.
Nieto, J.M., Almodóvar, G.R., Pascual, E., Sáez, R., Jagoutz, E., 2000. Evidencias isotópicas sobre el origen de los metales en los sulfuros masivos de la Faja Pirítica Ibérica. Cad Lab Xeol Laxe 25, 139–142.
Nocete, F., Álex, E., Nieto, J.M., Sáez, R., Bayona, M.R., 2005. An archaeological approach to regional environmental pollution in the South-Western Iberian Peninsula related to Third Millennium BC mining and metallurgy. J Archaeol Sci 32, 1566–1576.
Oliveira, J.T., 1990. South Portuguese Zone. 1. Introduction. 2. Stratigraphy and synsedimentary tectonism. In: Dallmeyer, R.D., Martínez García, E. (Eds.), Pre-Mesozoic Geology of Iberia. Springer, Berlin, Heidelberg, New York.
Oliveira, D.P.S., Matos, J.X.M., Rosa, C.J.P., Rosa, D.R.N., Figueiredo, M.O., Silva, T.P., Guimarães, F., Carvalho, J.R.S., Pinto, Á.M.M., Relvas, J.R.M.S., Reiser, F.K.M., 2011. The Lagoa Salgada Orebody, Iberian Pyrite Belt, Portugal. Econ Geol 106, 1111–1128.
Pirajno, F., Burlow, R., Huston, D., 2010. The Magellan Pb deposit, Western Australia: a new category within the class of supergene non-sulphide mineral systems. Ore Geol Rev 37, 101–112.
Relvas, J.M.R.S., Tassinari, C.C.G., Munhá, J., Barriga, F.J.A.S., 2001. Multiple sources for ore-forming fluids in the Neves Corvo VHMS deposit of the Iberian Pyrite Belt (Portugal): strontium, neodymium and lead isotope evidence. Miner Deposita 36, 416–427.
Roca, A., Viñals, J., Arranz, M., y Calero, J., 1999. Characterization and alkaline decomposition/cyanidation of beudantite–jarosite materials from Rio Tinto Gossan Ores. Can Metall Q 38, 93–103.
Routhier, P., Aye, F., Boyer, C., Lécolle, M., Moliere, E.P., Picot, P., Roger, G., 1978. La Ceinture Sud-Ibérique à amas sulfuré s dans sa partie espagnole mediane. Mém BRGM 94 (265 pp.).
Ruiz de Almodóvar, G., Sáez, R., 1992. Los yacimientos de sulfuros masivos de la Faja Pirítica Sur Ibérica. In: García Guinea, J., Martínez Frías, J. (Eds.), Recursos Minerales de España. C.S.I.C., Madrid.
Ruiz, C., Arribas, A., Arribas, A.J.R., 2002. Mineralogy and geochemistry of the Masa Valverde blind massive sulphide deposit, Iberian Pyrite Belt (Spain). Ore Geol Rev 19, 1–22.
Saéz, R., Almodóvar, G.R., Pascual, E., 1996. Geological constraints on massive sulphide genesis in the Iberian Pyrite Belt. Ore Geol Rev 11, 429–451.
Sáez, R., Pascual, E., Toscano, M., Almodóvar, G.R., 1999. The Iberian type of volcano-sedimentary massive sulfide deposits. Miner Deposita 34, 549–570.
Sáez, R., Nocete, F., Nieto, J.M., Capitán, M.A., Rovira, S., 2003. The extractive metallurgy of copper from Cabezo Juré, Huelva, Spain: chemical and mineralogical study of slags dated to the Third Millenium B.C. Can Mineral 41, 627–638.
Sato, M., 1960. Oxidation of sulfide ore bodies: I Geochemical environments in terms of Eh and pH. Econ Geol 55, 928–961.
Sato, M., 1992. Persistency-field Eh-pH diagrams for sulfides and their application to supergene oxidation and enrichment of sulfide ore bodies. Geochim Cosmochim Acta 56, 3133–3156.
Saunders, J.A., 1993. Supergene oxidation of bonanza Au–Ag veins at the Sleeper Deposit, Nevada, USA: implications for hydrochemical exploration in the Great Basin. J Geochem Explor 47, 359–375.
Schermerhorn, L.J.G., 1971. An outline stratigraphy of the Iberian Pyrite Belt. Bol Geol Min 82, 239–268.
Schoell, M., 1979. The hydrogen and carbon isotopic composition of methane from natural gases of various origins. Geochim Cosmochim Acta 44, 649–661.
Scott, K.M., Ashley, P.M., Lawie, D.C., 2001. The geochemistry, mineralogy and maturity of gossans derived from volcanogenic Zn–Pb–Cu deposits of the eastern Lachlan Fold Belt, NSW, Australia. J Geochem Explor 72, 169–191.
Sierro, F.J., González-Delgado, J.A., Dabrio, C.J., Flores, J.A., Civis, J., 1990. The Neogene of the Guadalquivir Basin (SW Spain). Paleontol Evolució Mem Esp 2, 209–250.
Sillitoe, R.H., 2005. Supergene oxidized and enriched porphyry copper and related deposits. In: Hedenquist, J.W., Thompson, J.F.H., Goldfarb, R.J., Richards, J.P. (Eds.), Economic Geology 100th Anniversary Volume. Society of Economic Geologists, Littleton, CO, pp. 723–768.
Silva, J.B., Oliveira, J.T., Ribeiro, A., 1990. South Portuguese zone. Structural outline. In: Dallmeyer, R.D., Martinez Garcia, E. (Eds.), Pre-Mesozoic Geology of Iberia. Springer-Verlag, Berlin, pp. 348–362.
Simancas, J.F., 1983. Geología de la extremidad oriental de la Zona Surportuguesa: Unpublished PhD Thesis. University of Granada, Spain.
Singer, P.C., Stumm, W., 1970. Acidic mine drainage, the rate-determining step. Science 167, 1121–1123.
Strauss, G.K., Madel, J., 1974. Geology of massive sulfide deposits in the Spanish–Portuguese Pyrite Belt. Geol Rundsch 63, 191–211.
Strauss, G.K., Madel, J., Fernández-Alonso, F., 1977. Exploration practice for strata-bound volcanogenic sulfide deposits in the Spanish–Portuguese Pyrite Belt. In: Klemm, D.D., Schneider, H.J. (Eds.), Time and Strata-bound Ore Deposits (Berlin, Heidelberg, New York).
Strauss, G.K., Roger, G., Lécolle, M., Lopera, E., 1981. Geochemical and geological study of the volcano-sedimentary sulfide orebody of La Zarza, Huelva Province. Spain Econ Geol 76, 1975–2000.
Stroffregen, R., 1986. Observations on the behaviour of Au during supergene oxidation at Summitville, Colorado, USA and implications for electrum stability in the weathering environment. Appl Geochem 2, 549–558.

Please cite this article as: Yesares, L., et al., The Las Cruces deposit, Iberian Pyrite Belt, Spain, Ore Geol. Rev. (2014), http://dx.doi.org/10.1016/j.oregeorev.2014.10.019

Stumm, W., Morgan, J.M., 1996. Aquatic Chemistry, 3rd. John Wiley & Sons, New York (pp).
Taylor, R., 2011. Gossans and Leached Cappings. Field Assessment. Springer, Berlin (146 pp).
Taylor, G.F., Thornber, M.R., 1992. Gossan and ironstone surveys. In: regolith exploration geochemistry in tropical and subtropical terrains. In: Butt, C.R.M., Zeegers, H. (Eds.), Handbook of Exploration Geochemistry. Elsevier, Amsterdam-London-New York-Tokyo.
Thiéblemont, D., Pascual, E., Stein, G., 1998. Magmatism in the Iberian Pyrite Belt: petrological constrains on a metallogenic model. Miner Deposita 33, 98–110.
Thornber, M.R., 1985. Supergene alteration of sulphides, VII. Distribution of elements during the gossan-forming process. Chem Geol 53, 279–301.
Thornber, M.R., Wildman, J.E., 1984. Supergene alteration of sulphides, VI. The binding of Cu, Ni, Zn, Co and Pb with iron-bearing gossan minerals. Chem Geol 44, 399–434.
Tornos, F., 2006. Environment of formation and styles of volcanogenic massive sulfides: the Iberian Pyrite Belt. Ore Geol Rev 28, 259–307.
Tornos, F., Barriga, F., Marcoux, E., Pascual, E., Pons, J.M., Relvas, J., Velasco, F., 2000. The Iberian Pyrite Belt. In: Large, R.R., Blundell, D.J. (Eds.), Database on Global VMS Districts, Codes-Geode, pp. 19–52.
Tornos, F., Velasco, F., Menor-Salván, C., Delgado, A., Slack, J., Escobar, J.M., 2014. Formation of recent Pb–Ag–Au mineralization by potential sub-surface microbial activity. Nat Commun 5, 1–8.
Velasco, F., Herrero, J.M., Suárez, S., Yusta, I., Alvaro, A., Tornos, T., 2013. Supergene features and evolution of gossans capping massive sulphide deposits in the Iberian Pyrite Belt. Ore Geol Rev 53, 181–203.
Viallefond, L., 1994. Cluster analysis on Geochemical results from gossans. In: Leistel, et al. (Eds.), The Massive Sulphide Deposits of the South Iberian Pyrite Province: Geological Setting and Exploration Criteria: BRGM. Doc, pp. 171–182.
Viñals, J., Roca, A., Cruells, M., Nuñez, C., 1995. Characterisation and cyanidation of Rio Tinto Gossan Ores. Can Metall Q 34, 115–122.
Williams, D., 1950. Gossanized breccia-ores, jarosites and jaspers at Rio Tinto Spain. Trans Inst Min Metall 526, 1–12.
Yesares, L., Nieto, J.M., Sáez, R., Almodóvar, G.R., Videira, J.C., 2010. El gossan de Las Cruces (FPI): Litología y evolución mineralógica. Macla 13, 225–226.
Yesares, L., Sáez, R., Nieto, J.M., Almodóvar, G.R., Stephen Cooper, S., 2014. Supergene enrichment of precious metals by natural amalgamation in the Las Cruces weathering profile (Iberian Pyrite Belt, SW Spain). Ore Geol Rev 58, 14–26.

Please cite this article as: Yesares, L., et al., The Las Cruces deposit, Iberian Pyrite Belt, Spain, Ore Geol. Rev. (2014), http://dx.doi.org/10.1016/j.oregeorev.2014.10.019